National Library
of Canada

Acquisitions and
Bibliographic Services Branch

395 Wellington Street
Ottawa, Ontario
K1A 0N4

Bibliothèque nationale
du Canada

Direction des acquisitions et
des services bibliographiques

395, rue Wellington
Ottawa (Ontario)
K1A 0N4

Your file Votre référence

Our file Notre référence

NOTICE

The quality of this microform is heavily dependent upon the quality of the original thesis submitted for microfilming. Every effort has been made to ensure the highest quality of reproduction possible.

If pages are missing, contact the university which granted the degree.

Some pages may have indistinct print especially if the original pages were typed with a poor typewriter ribbon or if the university sent us an inferior photocopy.

Reproduction in full or in part of this microform is governed by the Canadian Copyright Act, R.S.C. 1970, c. C-30, and subsequent amendments.

AVIS

La qualité de cette microforme dépend grandement de la qualité de la thèse soumise au microfilmage. Nous avons tout fait pour assurer une qualité supérieure de reproduction.

S'il manque des pages, veuillez communiquer avec l'université qui a conféré le grade.

La qualité d'impression de certaines pages peut laisser à désirer, surtout si les pages originales ont été dactylographiées à l'aide d'un ruban usé ou si l'université nous a fait parvenir une photocopie de qualité inférieure.

La reproduction, même partielle, de cette microforme est soumise à la Loi canadienne sur le droit d'auteur, SRC 1970, c. C-30, et ses amendements subséquents.

Canada

Flutter and Forced Aileron Oscillation analyses of an aircraft wing including the effect of the Nonlinear Wing-Fold Hinge

(Short Title: Forced Aileron Oscillation of a wing with Nonlinear Wing-Fold Hinge)

by

Mahendra VERMAUT

Under the supervision of Professor S.J.Price

A Thesis submitted to the Faculty of Graduate Studies and Research
in partial fulfillment of the requirements
for the degree of Master of Engineering

Department of Mechanical Engineering
McGill University, Montreal

May 1994

ISBN 0-315-99988-8

ACKNOWLEDGEMENT

The author gratefully acknowledges the guidance and advice offered by Prof. S.J. Price throughout the course of this study, as well as his continued support and encouragement which have been essential to the completion of the thesis.

Acknowledgement is also given to the Institute of Aerospace Research (formerly National Aeronautical Establishment) of Canada who financed this research under contract number 055SS.31946-8-0014.

ABSTRACT

A methodology is presented to calculate the response of a wing as well as the aerodynamic forces on the wing, due to forced aileron oscillations. The purpose of oscillating the ailerons in flight is to excite the vibration modes of the wing. From vibration recordings and knowledge of the aerodynamic forces induced by the aileron oscillation, the vibration modes of the wing can be *identified*. Identified modes may then be compared to wing vibration modes which are *calculated* through aeroelastic analyses of the wing. In particular, the flutter characteristics of the wing, predicted through aeroelastic analyses, can be verified.

The flutter and forced aileron oscillation analyses are performed on the aeroelastic equations built for a finite-element model of the wing. An existing finite-element model is used. The aerodynamic forces induced by wing vibrations are calculated through the doublet-lattice method, using existing software. The flutter and forced aileron oscillation analyses are based on the modal form of the aeroelastic equations. The modal transformation and the resulting equations are rigourously outlined. A physical interpretation of the mathematical formulae is given.

In particular, the effect of the nonlinear wing-fold hinge is addressed. In order to maintain linear aeroelastic equations, the nonlinear hinge characteristic is linearized. This imposes an iterative solution of the aeroelastic equations.

Sample flutter calculations are performed for different values of the equivalent linear wing-fold hinge stiffness. The P-k method is used. Extensive studies of the effect of structural nonlinearities on wing flutter behaviour are described in the literature.

The study of forced aileron oscillations was the main part of the thesis. The equations

and the iterative algorithm are built. The wing response and aerodynamic forces are calculated for different values of flight parameters, and the aileron oscillation amplitude and frequency. The effect of the structural nonlinearity is addressed, as well as the effect of the wing flexibility and the number of modes retained in the equations.

Although some interesting conclusions could be drawn from the results, further work of evaluating the accuracy of results is required. Another suggested topic for future work is the study of modal identification methods, and their integration with the work described here.

The analysis in this thesis represents a generic analysis of an aircraft, and thus only normalized numerical values are given.

SOMMAIRE

Une méthodologie est présentée pour calculer la réponse d'une aile, ainsi que les forces aérodynamiques correspondantes, résultant d'une oscillation imposée des ailerons. L'oscillation des ailerons a pour but d'exciter les modes propres de vibration de l'aile, afin d'identifier ces modes. On peut ensuite comparer les modes identifiés aux modes correspondants calculés par des calculs fluidélastiques de l'aile. En particulier, des prédictions de modes instables de vibration peuvent être verifiées.

Dans le présent travail, les prédictions d'oscillations fluidélastiques instables, ainsi que les calculs de la réponse de l'aile aux oscillations imposées des ailerons, sont basés sur un modèle éléments-finis de l'aile. Un modèle existant est utilisé, ainsi qu'une méthode existante ('doublet lattice method') pour calculer les forces aérodynamiques oscillatoires. Tous les calculs sont basés sur la forme modale des équations fluidélastiques. La transformation modale et les équations résultantes sont présentées de manière rigoureuse.

En particulier, l'effet d'une nonlinéarité dans le modèle structurel est adressé. Pour maintenir des équations linéaires, la nonlinéarité est remplacée par un élément linéaire correspondant. Ceci impose une solution itérative aux équations.

Des analyses de prédiction d'instabilités fluidélastiques sont décrites en détail dans la litérature, pour l'aile étudiée dans le présent travail, et ont permis une comparaison avec des résultats obtenus dans ce travail.

La plus grande partie du présent travail a consisté en l'étude des oscillations forcées des ailerons. Les équations et la solution itérative sont décrits. La réponse de l'aile et les forces aérodynamiques correspondantes sont calculées pour différentes valeurs des paramètres du vol, et de l'amplitude et la fréquence d'oscillation des ailerons. Les effets de la nonlinéarité

structurelle, de la flexibilité de l'aile, et du nombre de modes vibratoires sont quantifiés.

Si l'auteur a formulé certaines conclusions, il suggère aussi des voies futures de travail: études de sensitivité pour quantifier l'erreur; une analyse des méthodes d'identification de modes vibratoires, et de l'intégration avec le présent travail.

La présente analyse représente une analyse générique d'une aile, et ne donne que des résultats normalisés.

USED DESIGNATIONS

$\{F_a(t)\}$	Vector of forcing terms in the direct equations of motion.
$\{F(t)\}$	Vector of modal generalised forces.
$\{F_{aero}(t)\}$	Vector of aerodynamic induced modal forces.
$\{F_{ail}(t)\}$	Vector of modal forces due to imposed aileron oscillation.
$\{u_a(t)\}$	Vector of grid point displacements in the finite-element model of the wing.
$\{A(t)\}$	Vector of modal amplitudes.
$\{U_a\}$	Mode shape vector in terms of direct coordinates.
$\{\overline{A}\}$	Vector of complex modal amplitudes for oscillatory wing motion.
A_F	Amplitude of forced aileron oscillation.
$\{\phi\}_i$	i-th wing natural mode.
$[\Phi]$	Modal matrix of the wing.
$[M_{aa}]$	Direct mass matrix of the wing.
$[K_{aa}]$	Direct stiffness matrix of the wing.
$[M]$	Modal mass matrix of the wing.
$[K]$	Modal stiffness matrix of the wing.
$[D]$	Modal damping matrix of the wing.
$[Q_i]$	Imaginary part of the matrix of aerodynamic induced modal forces.
$[Q_r]$	Real part of the matrix of aerodynamic induced modal forces.
n	Number of degrees of freedom in the finite-element model of the wing.

Contents

Chapter 1

Introduction

This chapter gives a description of the purpose and subject of the thesis, including

- the aircraft wing structural analysis;
- the modal aeroelastic equations (wing-flow interaction equations) and the flutter instability analysis;
- forced aileron oscillations of the wing for in-flight testing of the analytically obtained wing oscillation modes;
- the effect of the nonlinear wing-fold hinge on above analyses.

This first chapter is mainly descriptive. Detailed analytical elaboration of each of the subjects is given in the following chapters.

1.1 Purpose of the Study

The purpose of the thesis is

- to accurately describe a methodology to calculate the wing motion and aerodynamic forces due to forced aileron oscillations;
- to implement the methodology, using both the flutter analysis software available at the National Aeronautical Establishment (now Institute of Aerospace Research), and programs written for this thesis at the McGill University;
- to perform example calculations for a limited set of wing configurations and flight parameter values, to assess the feasibility of the method as well as of the interpretation of the results;
- to compare the methodology and results with reference [4], where applicable.

1.2 Subject of the Study

A structural analysis of the aircraft wing is performed using the finite-element method. This analysis yields eigenfrequencies of the wing, with corresponding eigenmodes.

Any deflection of the wing can be written as a linear combination of eigenmodes. The coefficients in this linear combination are referred to as the modal amplitudes.

Equations of motion of the wing are then constructed. One of the possible forms in which these equations can be written is in terms of these modal amplitudes. This modal form of the equations is convenient for two main reasons:

- aerodynamic forcing terms in the equations will be conveniently calculated as *modal forces*;
- the modal form allows a reduction of the order of the system of equations of motion. The order of the equations of motion as obtained from the finite-element analysis is indeed too large (equal to the number of degrees of freedom in the finite-element model, or approximately 150 for the wing model) to be computationally cost-effective in an iterative solution process. A reduction of the order of the equations by considering only the most important contributing *modes* makes calculations tractable, concentrates the effort on the most important contributions, and is likely to provide acceptable results in a frequency range of interest.

Forcing terms are added to the structural equations of motion of the wing. These forcing terms are added in two successive steps.

- When a vibrating wing, or structure in general, is placed in a fluid flow, forces of the flow on the structure are altered by the oscillation of the structure. In other words, a *dynamic*, oscillating force is induced on the structure by the oscillation of this structure. The equations of motion of the wing which include these oscillatory

forces due to the interaction between the structure and the flow, are the *aeroelastic equations of motion.* An analysis of the aeroelastic equations provides stability data of the structure-flow system. The occurrence of dynamic instability is referred to as *wing flutter.*

- In a second step, *external* (other than the induced aerodynamic forces) forces are added to the aeroelastic equations. For the study described here, external forces are imposed on the wing for experimental verification of theoretical flutter predictions via flight tests. The external forces are induced on the wing by forced aileron oscillations.

Flutter is a violent and dangerous instability. Under certain flight conditions, a slight oscillation can induce aerodynamic forces which help the initial oscillation to grow exponentially. The airspeed is the most important parameter influencing the occurrence of flutter. Flutter typically occurs above a given airspeed. The flight speed should be kept lower than this critical airspeed, with some safety margin.

Theoretical flutter calculations are based on approximate models of the structure and the aerodynamic forces, as well as approximations in the calculations (e.g. reduction of the order of the system of equations). Results must be verified via flight tests. In these flight tests, an excitation is applied to the aircraft wing in flight. From measured responses, one can identify modes and their frequency and damping, and compare them to theoretically predicted modes at the same flight conditions. In some flight tests, the external excitation is provided by oscillating the ailerons [2]. The aileron oscillation induces aerodynamic forces on the wing. In this thesis, we calculate the deflection of the wing resulting from the aileron oscillation, and the exact aerodynamic forces induced by it.

The flutter analysis method we use is linear. This requires a linear structural model and linear expressions for induced aerodynamic forces. Nevertheless, we want to study the

effect of an important nonlinearity in the wing structure: the wing-fold hinge. The hinge characteristic shows a freeplay zone around its zero-deflection position. A describing-function technique is used to linearize the hinge, by introducing an *equivalent* linear hinge stiffness. This equivalent stiffness is defined for an oscillatory deflection of the hinge, and is a function of the oscillation amplitude. The structural nonlinearity has an effect on flutter analysis results. Also, studying the effect of the structural nonlinearity on the response to forced aileron oscillation involves an iterative procedure of solving the equations for successive values of the equivalent stiffness.

The following sections of this chapter help to understand the methods used. A formal and detailed elaboration of formulas and methods, as well as results of the study are found in the following chapters.

1.3 Aeroelastic Equations

In order to obtain the aeroelastic equations of motion, we first construct the structural equations of motion. The aeroelastic equations, or wing-flow interaction equations, are then obtained by introducing the aerodynamic forces induced by structural vibrations. In a finite-element model of the wing, a motion of the continuous structure is reduced to displacements (both translations and rotations) of a discrete number of grid points. The possible independent displacements of grid points are referred to as *degrees-of-freedom.* Forces on the wing are expressed as forces and torques applied at the grid points. Any oscillatory deformation mode of the wing induces oscillatory aerodynamic forces acting at the grid points, with a certain amplitude and phase difference with respect to the initial oscillation.

1.3.1 Structural Equations

The structural equations of motion for the finite-element model of the wing are of the form

$$[M_{aa}]\{\ddot{u}_a\} + [K_{aa}]\{u_a\} = \{F_a\}. \tag{1.1}$$

$\{u_a\}$ is the vector of independent displacements (translations or rotations) at grid points, referred to as degrees-of-freedom. $\{F_a\}$ is the vector of external forces applied at grid points. The number of components of both vectors is equal to the number of degrees-of-freedom in our finite-element model of the wing. The wing model used in this thesis had approximately 150 degrees-of-freedom.

Figure 1.2 shows a simple structure suspended in a fluid flow. The structure has a very limited number of degrees-of-freedom. The rigid wing section, suspended from a spring, can translate vertically and rotate in pitch. The aileron can rotate. The simplified model is interesting for understanding phenomena. The occurrence of flutter, for example,

can be studied. Indeed, when the model is placed in an airflow and induced aerodynamic forces are introduced in the equations, dynamic instability (flutter) is predicted by the equations. The number of parameters which define the model of the plate (mass, stiffness of suspending springs, location of center of gravity and spring attachments) is small. The effect of each of these parameters on the occurring phenomena can therefore be studied and provides useful *qualitative* information.

The purpose of the study described in this thesis is different. We use a more complete model of the wing, with a higher number of degrees-of-freedom (the real wing is a continuous structure, and has an infinite number of degrees-of-freedom), in order to obtain *quantitative* values which are more accurate predictions of wing oscillation parameters, aerodynamic forces, ...The wing is represented via a finite element model. The structural part of this model is not the main topic of this thesis, and thus details are not given here. The main elements are elastic beam elements, which together span the 2-dimensional surface of the wing. Other elements are rigid connections, hinges, ... Each element imposes relationships between the degrees-of-freedom of the grid points which it connects, and forces (both external and internal) applied at these grid points. The wing inertia is modelled as concentrated masses attached to the grid points. Through matrix manipulations, the equations of the individual elements are combined to form equations (1.1) in the independent degrees-of-freedom, after elimination of constraints and internal forces. The equations are linear, as they are based on a linear model. Matrices $[M_{aa}]$ and $[K_{aa}]$, the mass and stiffness matrices respectively, are in general nondiagonal matrices.

1.3.2 Modal Aeroelastic Equations

In flight, any deflection $\{u_a\}$ of the wing induces aerodynamic forces $\{F_a\}$ at grid points on the wing.

In order to build the aeroelastic equations, the induced aerodynamic forces must be

expressed as functions of grid point displacements.

Let n be the number of degrees-of-freedom of the wing. A wing deflection is a vector of dimension n. For the n-dimensional space, one can construct a set of independent vectors spanning the n-space (basis vectors). Any deflection can then be written as a linear combination of these vectors.

Linearity of induced aerodynamic forces assumes that the aerodynamic force induced by a deflection is given by the same linear combination of the aerodynamic forces induced by the basis vectors.

The set of vectors typically chosen for spanning the n-space of deflections is the set of natural modes of vibration of the wing, or eigenvectors of the structural equations of motion. This is a good choice for several reasons:

- eigenmodes satisfy the boundary conditions, as they are obtained from a set of equations consisting of both the wing dynamics and its boundary constraints.
- a coordinate transformation to this set of basis vectors yields *diagonal* mass and stiffness matrices.
- eigenmodes of the wing reflect the natural deflections of the wing. Even if an external force (e.g. the induced aerodynamic forces) will not deflect the wing in one of its natural modes but rather a linear combination of eigenmodes, a number of modes in this linear combination will be dominant and others negligible. This will allow a reduction of the order of the system, saving computational costs.
- eigenmodes are 'smooth' natural modes. This makes the assumption that induced aerodynamic forces can be obtained as a linear combination of contributions from individual eigenmodes, acceptable.

It will be convenient to *transform* the direct equations of motion (1.1) to a new coordinate system. The spanning vectors for the new system are the set of n eigenmodes

of the wing. Vectors of grid point displacements are transformed to vectors of *modal amplitudes.* Mathematical details of the transformation are given in Chapters 2 and 4. After transformation, the equations of motion take the form

$$[M]\{\ddot{A}\} + [K]\{A\} = \{F\}.$$

The modal mass matrix $[M]$ and the modal stiffness matrix $[K]$ are now diagonal. The right hand side of the equations is the vector of modal forces. External forces, e.g. the induced aerodynamic forces, are expressed as *modal forces.* A deflection in any of the natural modeshapes induces aerodynamic forces. As the wing motions which we consider are *sinusoidal,* both for flutter analysis and for the response of the wing to forced aileron oscillation, expressions for the aerodynamic forces can be restricted to periodic motion. The aerodynamic forces induced by a periodic oscillation of the wing are calculated numerically.

1.3.3 Aerodynamic Forces

The aerodynamic forces are calculated as modal forces. The modal aerodynamic forces represent how an oscillation of the wing in one mode induces forces on itself and each of the other modes:

$$\{F\} = [Q_r]\{A\} + [Q_i]\{\dot{A}\}.$$

The matrices $[Q_r]$ and $[Q_i]$ are *nondiagonal* matrices of components of modal aerodynamic forces, respectively in phase and out of phase with the modal deflection.

It will be important to realise that the modal aerodynamic forces *depend on the frequency of the oscillation by which they are induced.*

The modal aerodynamic forces are obtained through a numerical method referred to as the 'doublet lattice method'. The method is described in [1].

Structural equations and aerodynamic forces taken together yield the modal aeroe-

lastic equations

$$[M]\{\ddot{A}\} - [Q_i]\{\dot{A}\} + ([K] - [Q_r])\{A\} = \{0\}. \tag{1.2}$$

1.4 Flutter Analysis

The aeroelastic equations (1.2) are a set of homogeneous linear differential equations. A flutter analysis consists of a *stability analysis* of this set of equations.

1.4.1 Stability Analysis: Characteristic Equation Method

We assume solutions of the form

$$\{A(t)\} = \{\overline{A}\}e^{\lambda_r t}\sin\lambda_i t. \tag{1.3}$$

This represents a damped oscillation. λ_i is the angular frequency. λ_r is a measure of the damping; positive damping corresponds to a negative λ_r. $\{\overline{A}\}$ represents the complex shape of oscillation. By introducing the complex notation, this can be written as

$$\{\overline{A}\}e^{\lambda t}, \tag{1.4}$$

where $\lambda = \lambda_r + j.\lambda_i$. Substituting (1.4) in (1.2) yields

$$\left[\lambda^2[M] - \lambda[Q_i] + [K] + [Q_r]\right].\{\overline{A}\} = \{0\}. \tag{1.5}$$

A nontrivial solution, $\{\overline{A}\} \neq 0$, to equations (1.5) can only exist for values of λ for which

$$\left|\lambda^2[M] - \lambda[Q_i] + [K] + [Q_r]\right| = 0. \tag{1.6}$$

This equation in λ is called the characteristic equation.

For each $\lambda = \lambda_r + j.\lambda_i$, solution of the characteristic equation, (1.5) becomes a set of n algebraic equations in the components of $\{\overline{A}\}$. $n-1$ equations are linearly independent. One component of the vector can be chosen freely. The other $n-1$ components can then be calculated, determining the 'shape' corresponding to that particular λ. When initial conditions are added to the system of differential equations (1.2), these will uniquely determine all components of $\{\overline{A}\}$. The initial-value-problem has a unique solution in time, starting from the initial condition.

The stability of any such solution can be studied from the set of homogeneous equations (1.2), independently of initial conditions. The *stability* is determined by the λ values obtained by solving the characteristic equation. As the characteristic equation has real coefficients, solutions are either real or complex conjugate pairs. The system is stable if all λ-s have negative real part λ_r. Indeed, it can be seen from (1.3) that if λ_r is negative, the amplitude of the oscillation is damped exponentially.

If one λ has positive real part, the system is unstable. The structure will start to oscillate, as soon as the slightest disturbance occurs, with an exponentially increasing amplitude. The 'shape' of the oscillation is given by the $\{\overline{A}\}$ which corresponds to the unstable λ.

1.4.2 Stability Analysis: Eigenvalue Method

Solving the characteristic equation is computationally very expensive and becomes untractable for a large order of the matrices. The eigenvalue method is a more efficient way of calculating λ-s and $\{\overline{A}\}$-s. The eigenvalue problem occurs very often in applied mathematics, and efficient algorithms to solve it have been developed.

In order to formulate the stability analysis as an eigenvalue problem, the set of second order differential equations must be transformed into an extended set of first order equations. We define a *state vector* as

$$\{A_{st}\} = \{ \begin{matrix} A \\ \dot{A} \end{matrix} \}.$$

One can verify that

$$\begin{bmatrix} [I] & [0] \\ [0] & [M] \end{bmatrix} \begin{pmatrix} \dot{A} \\ \ddot{A} \end{pmatrix} + \begin{bmatrix} [0] & -[I] \\ [K] & [Q_d] & -[Q_i] \end{bmatrix} \begin{pmatrix} A \\ \dot{A} \end{pmatrix} = \{0\}$$

is a correct set of equations. It can be rewritten as

$$[C]\{\dot{A}_{st}\} + [D]\{A_{st}\} = \{0\}. \tag{1.7}$$

Intoducing $\{A_{st}(t)\} = \{\overline{A}_{st}\}e^{\lambda t}$ in the same way as we did for the characteristic equation method, substitution into (1.7) yields

$$\Big[\lambda.[C] + [D]\Big]\{\overline{A}_{st}\} = \{0\}.$$

Finding λ-values for which a nontrivial solution for $\{\overline{A}_{st}\}$ exists, is an eigenvalue problem. λ-values are *eigenvalues*, the corresponding $\{\overline{A}_{st}\}$ vectors are *eigenvectors*. Efficient algorithms exist for solving the eigenvalue problem.

Eigenvalues are real or complex conjugate numbers. The eigenvalues determine the stability of the system. For stability, *all* eigenvalues must have negative real part.

1.4.3 Flutter

The matrices of induced aerodynamic forces depend on a number of flight parameters, such as Mach number and (equivalent) airspeed. Assuming for instance a constant Mach number, the matrices depend on the equivalent airspeed, through the dynamic pressure

$$p_{dyn} = \frac{1}{2}\rho_0 V_{EAS}^2.$$

For each value of the equivalent airspeed, matrices of modal induced aerodynamic forces can be calculated, and substituted in the aeroelastic equations. The eigenvalues of the sytem can then be calculated. These eigenvalues determine the stability of the system. Therefore, the stability depends on the equivalent airspeed.

Typically, a wing will be stable for sufficiently low airspeeds. For this stable case, external excitations are damped due to the interaction between structure and flow. As

the airspeed increases, the real part of some eigenvalues can become positive, and hence the system becomes unstable. The interaction between the structure and the flow has become such that oscillations of the wing induce aerodynamic forces which help the initial oscillation to grow.

As already mentioned, the work in this thesis assumes a model of the wing which is sufficiently complete to provide quantitative results. Nevertheless, a qualitative understanding of the occurrence of flutter can be obtained from simple models of a 'wing', reduced to a rigid wing section flexibly mounted, with two degrees of freedom: vertical translation and rotation in pitch (Figure 1.2, without aileron rotation). For zero airspeed, the aeroelastic equations are purely structural. For the two degree-of-freedom model, two uncoupled modes of oscillation can be found at this zero airspeed: one represents a vertical translation, the other a rotation in pitch about a given point. As the airspeed increases, the aerodynamic forces can cause modes to become coupled. Each mode is a combination of vertical motion and pitch. The most important coupling is the variation in lift, acting in the vertical direction, due to the variation in angle of attack of the flow on the wing, caused by its oscillation in pitch. Whether a mode, now a combination of vertical motion and pitch, becomes unstable will depend on the phase difference between pitch and vertical motion within that mode.

It can be demonstrated from the analysis of the above simple model that:

- flutter is a dynamic instability involving at least two structural modes (more general forms of flutter which can occur with only one mode - especially when unsteady effects are accounted for, are not addressed by the simplified linearized theory of this thesis);
- interaction between two structurally independent modes is due to induced aerodynamic forces;
- a (combined) mode becomes unstable when the corresponding eigenvalue has posi-

tive real part (i.e. negative damping). This occurs above a critical airspeed. Flutter is also called a 'frequency coalescence' instability, as frequencies of two modes tend towards each other for airspeeds close to the critical value. This is another indication that these two modes 'operate together' in causing the instability.

This same 'flutter behaviour' will be illustrated by the flutter analysis results of Chapter 3, based on the more complete wing model used in this thesis. Frequencies of two of the structural modes will tend towards each other as the airspeed increases. These modes are the contributing modes in the flutter mechanism. They correspond essentially to a wing-pitch mode and a wing-bending mode.

1.4.4 P-k Method for Flutter Analysis

A flutter analysis consists of a stability analysis of the system of aeroelastic equations, for different values of the flight parameters.

For each set of the flight parameters which influence flutter, eigenvalues λ are calculated. In general, eigenvalues are complex numbers: $\lambda = \lambda_r + j.\lambda_i$. With each eigenvalue corresponds an oscillation mode of the wing. λ_i is the angular frequency of motion of that mode.

A difficulty arises in flutter analysis. Induced aerodynamic forces depend on the frequency of oscillation of the wing. More precisely, they depend on a 'reduced' (nondimensional) frequency defined as

$$f_{red} = \frac{f * c}{2 * V}$$

with c a reference length (e.g. the mean chord of the wing) and V the airspeed. The dependence becomes more important for large values of reduced frequency.

The matrices of aerodynamic forces (valid for *sinusoidal* motion) depend on the frequency of oscillation, hence on λ_i. However, the eigenvalues are precisely a result of

the set of equations, hence the aerodynamic matrices. Exact eigenvalues λ (or angular frequencies of oscillation λ_i) therefore have to be obtained iteratively:

- guess a value for the reduced frequency of the r-th mode;
- calculate the r-th eigenvalue or angular frequency;
- recalculate the reduced frequency from the angular frequency, and restart the iteration until the procedure converges;
- repeat this process for all the eigenvalues (or all modes).

This method is known as the P-k method. It is computationally expensive, as matrices of aerodynamic forces must be recalculated for each new reduced frequency during the iteration. In order to restrict the amount of calculation, aerodynamic forces are calculated for a number of reduced frequencies, referred to as 'hard reduced frequencies'. Aerodynamic matrices for any other reduced frequency are obtained by linear interpolation.

Flutter calculations in Chapter 3 were performed with the P-k method. Other methods exist for flutter analysis, as there are the simplified P-method, and the U-g method, for which we refer to the literature.

1.5 Flight Testing

1.5.1 System Identification

Flight testing referred to in this thesis aims at verifying the results of theoretical calculations: oscillation modes (frequency and shape) of the wing under given flight conditions as well as the potential of occurrence (or margin before occurrence) of flutter for varying flight conditions (equivalent airspeed, Mach number, aircraft configuration, ...).

An excitation is imposed on the wing and its response is recorded. From these recordings, vibration modes must be reconstructed, and their frequency and damping determined. The choice of the external excitation (excitation locations, frequency content, ...) and wing motion monitoring (recording locations), and the subsequent identification of modes (shape, frequency, damping) are the subject of extensive fields of study of vibration testing and modal identification, which are not further developed in this thesis. Refs. [2] and [3] are example publications on aircraft modal test programs and issues in the field of modal identification.

1.5.2 Flight Testing External Excitation

In flight tests, a wing may be excited by oscillating the ailerons. The excitation of the wing is due to aerodynamic forces which are induced by the aileron oscillation. In Chapter 4, the equations and methodology are outlined which permit to introduce the aileron oscillation forces into the equations of motion of the wing finite-element model previously developed. Results of sample calculations of induced forces on the wing are presented.

The aerodynamic forces induced by the imposed aileron oscillation are an input to the identification of wing vibration modes for given flight conditions, together with the

recorded wing response.

The induced force may be calculated in any form, depending on the requirements of different modal identification methods: either one total aerodynamic force on the wing, or a force distribution over the wing, corresponding to the layout of multiple recording points (e.g. accelerometers) on the wing.

The amplitude and frequency of the aileron oscillation can be varied.

1.6 Structural Nonlinearity

So far, linear structural equations have been assumed for a linear finite-element model of the wing. Also, expressions for the induced aerodynamic forces are linear. However, a main structural element in the wing, the wing-fold hinge, has an important nonlinearity. The characteristic of this hinge shows a freeplay zone.

Previous studies have shown that this nonlinearity has a considerable effect on the flutter characteristics of the wing.

The nonlinearity is also introduced in the analysis of the wing response to imposed aileron oscillations.

The wing-fold hinge characteristic is shown in Figure 1.1. $K1$ is the nominal stiffness of the hinge. Over a zone of $2S$, called the freeplay zone, the hinge stiffness $K2$ has a much lower value. S is referred to as the freeplay radius. Due to preloading of the hinge in flight, the freeplay zone is not located around the 'origin' of the characteristic. The preloading is measured by the parameter P.

Due to the nonlinearity, the deflection of the hinge to an assumed sinusoidal load will be periodic but asymmetric. The ratio between the hinge deflection amplitude and the amplitude of the applied sinusoidal torque is not constant (as it should be for a linear hinge). It depends on the location of the freeplay zone and varies with the amplitude of the applied load.

In order to maintain a linear model for flutter analysis, the nonlinear hinge must be linearized. The notion of *equivalent linear stiffness* is introduced.

1.6.1 Linearization: Describing Function Method

The describing function is a useful technique in treating structural nonlinearities by evaluating an equivalent stiffness. The dynamic system can be linearized and the usual linear

analysis methods can be applied. The basic approach for the method is to assume that the displacement is sinusoidal. The load developed in the nonlinear spring is expanded in a Fourier series. Only the first harmonic is retained, the higher harmonic terms are neglected.

Consider the harmonic deflection

$$x = X \sin \omega t,$$

of the hinge. The load (torque) which corresponds to this harmonic deflec-tion is in general not sinusoidal, due to the nonlinearity. Nevertheless, it is periodic, and can be expanded in a Fourier series of the form

$$f = F_0 + \sum_{n=1}^{\infty} (Fn \sin n\omega t + G_n \cos n\omega t).$$

The describing function is then defined as

$$DF = \frac{(F_1^2 + G_1^2)^{\frac{1}{2}}}{X} . e^{j\phi},$$

with

$$\phi = \tan^{-1}(\frac{G_1}{F_1}),$$

i.e. only the first harmonic in the Fourier series is retained. The equivalent linear stiffness of the hinge is defined as the amplitude of the describing function.

Amplitudes of the first harmonic components can be calculated from

$$F_1 = \frac{\omega}{\pi} \int_0^{\frac{2\pi}{\omega}} f(t) \sin \omega t dt,$$

and

$$G_1 = \frac{\omega}{\pi} \int_0^{\frac{2\pi}{\omega}} f(t) \cos \omega t dt,$$

using the correct expression for $f(t)$.

For the particular nonlinear spring characteristic shown in Figure 1.1, this depends on whether $X \leq P$, $P < X \leq P + 2S$ or $P + 2S < X$.

Example expressions for the case $P < X \leq P + 2S$ are

$$f(t) = K_1 X \sin \omega t \qquad for \quad x \leq P$$
$$f(t) = (K_1 - K_2)P + K_2 X \sin \omega t \quad for \quad P < x,$$

knowing that $P < x$ in a time interval $\tau_1 < t < \tau_2$ of the period $[0, \frac{2\pi}{\omega}]$, satisfying

$$X \sin \omega \tau_1 = P,$$
$$X \sin \omega \tau_2 = P,$$
$$\omega \tau_1 + \omega \tau_2 = \pi.$$

Reference [4] gives the formulas in their final form. The formulas are repeated hereafter. They are used to calculate the equivalent stiffness corresponding to a given hinge deflection, and for a given set of hinge parameters (K_1, K_2, P, S).

$$K_e = K_1, \quad \text{for } A \leq P$$
$$= \frac{1}{\pi}\left\{K_1\pi + (K_2 - K_1)t_1 + 2(K_1 - K_2)\left(\frac{P - A_0}{A_1}\right)\sin t_1 + \left(\frac{K_2 - K_1}{2}\right)\sin 2t_1\right\}, \quad \text{for } P \leq A \leq P + 2S$$
$$= \frac{1}{\pi}\left\{2(K_1 - K_2)\left(\frac{P - A_0}{A_1}\right)\sin t_1 + (K_2 - K_1)t_1 + 2(K_2 - K_1)\left(\frac{P + 2S - A_0}{A_1}\right)\sin t_2 + (K_1 - K_2)t_2 + \frac{K_2 - K_1}{2}(\sin 2t_1 - \sin 2t_2) + K_1\pi\right\}, \quad \text{for } A \geq P + 2S \quad (3)$$

where

$$t_1 = \cos^{-1}\left(\frac{P - A_0}{A_1}\right)$$
$$t_2 = \cos^{-1}\left(\frac{P + 2S - A_0}{A_1}\right)$$
$$A = A_0 + A_1$$
$$A_0 = 0, \quad A \leq P$$
$$= \frac{A}{2} - \frac{1}{2}\sqrt{A^2 - \frac{K_1 - K_2}{K_1}(P - A)^2}, \quad P \leq A \leq P + 2S$$
$$= \frac{A}{2} - \frac{1}{2}\sqrt{A^2 - 4S\left(\frac{K_1 - K_2}{K_1}\right)(A - P - S)}$$
$$A \geq P + 2S$$

1.6.2 Effect of the Structural Nonlinearity

The nonlinear wing-fold hinge is replaced by an equivalent linear hinge with equivalent linear stiffness. The equivalent stiffness, defined for an oscillatory hinge deflection, depends on the amplitude of oscillation.

In the finite-element model of the wing, the equivalent linear wing-fold hinge is used. Modal mass and stiffness matrices, modal frequencies and mode shapes are based on the model, and therefore depend on the equivalent stiffness.

Matrices of modal induced aerodynamic forces are constructed from the modeshapes. They also depend on the equivalent stiffness.

The nonlinearity of the wing-fold hinge influences the wing flutter analysis and the study of forced aileron oscillation.

- **Flutter Analysis.**

  As all matrices in the aeroelastic equations depend on the equivalent hinge stiffness, so do flutter analysis results. Flutter analysis is performed for a range of equivalent hinge stiffness values, lying between the low freeplay stiffness and the nominal stiffness.

  Detailed analyses of the influences of the equivalent hinge stiffness on wing flutter have been performed and are described in the literature [4]. Some results, though not the complete analysis, from [4] are reproduced in Chapter 3 of this thesis.

- **Forced Aileron Oscillation**

  As the aileron is oscillated with a given frequency and amplitude, the complete wing oscillates (with the same frequency) because of the induced aerodynamic forces. In particular, the wing-fold hinge assumes an oscillatory deflection with a certain amplitude. To this amplitude corresponds an equivalent hinge stiffness.

The equivalent stiffness therefore is a result of the forced aileron oscillation calculations. On the other hand, the equations of motion depend on the value of the equivalent stiffness. In order to calculate the response of the wing with the correct equivalent stiffness, the equations will have to be solved iteratively.

For given flight conditions (hence given preload on the wing-fold hinge), the equivalent hinge stiffness is determined by the forced aileron oscillation. The wing is then calculated to behave as if its wing-fold hinge were linear, with a stiffness equal to the equivalent stiffness. Modes obtained experimentally in flight tests must be compared to theoretical modes (obtained from flutter analysis) corresponding to that particular equivalent stiffness.

1.7 Computer Organisation

The computer programs for flutter analysis available at the National Aeronautical Establishment were used, as well as data manipulation and forced aileron oscillation analysis programs locally developed and run at the McGill University:

- the NASTRAN structural finite-element model was available.
- the above input file was adapted to include the wing-fold hinge stiffness, and perform the NASTRAN analyses.
- resulting wing modes and modal frequencies (masses, stiffnesses) were used in the calculation of the induced aerodynamic forces as well as the preformance of flutter analyses.
- matrices of generalized forces were transferred to McGill University for performing the forced aileron oscillation analyses.

1.8 Thesis Outline

The structural equations of motion, the modal transformation and resulting modal equations of motion are derived in Chapter 2. In Chapter 3, flutter analysis is illustrated. In particular, flutter analysis is performed for several values of the wing-fold hinge stiffness. Flutter analysis results are compared to [4]. Chapter 4 covers the study of forced aileron oscillation. The response of the wing to forced aileron oscillation is calculated, together with the aerodynamic forces induced on the wing by the aileron oscillation and the resulting wing motion. Chapter 5 summarizes the results, conclusions and further applicability of the work performed.

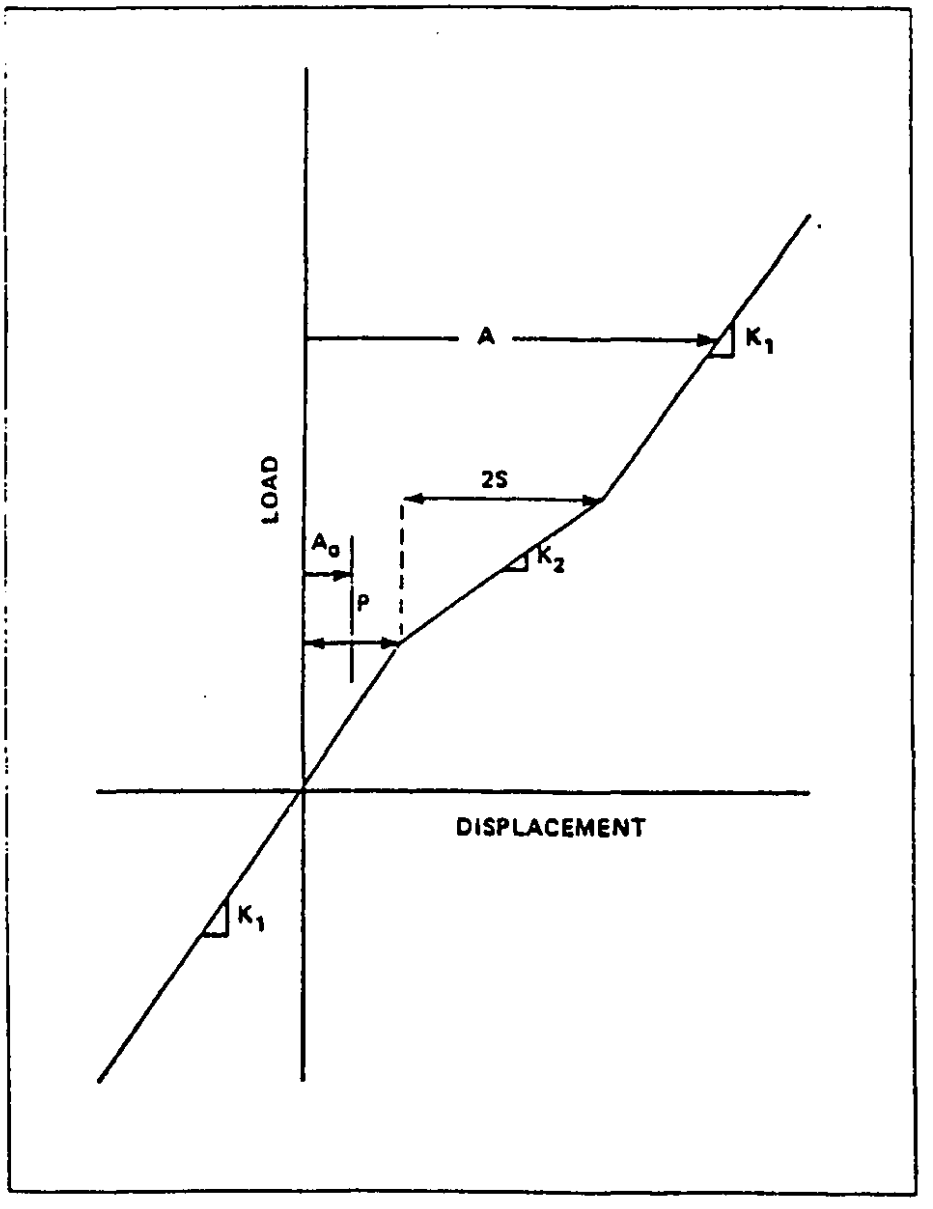

Figure 1.1

Moment-displacement function for CF-18 wing-fold hinge (source: Ref.7)

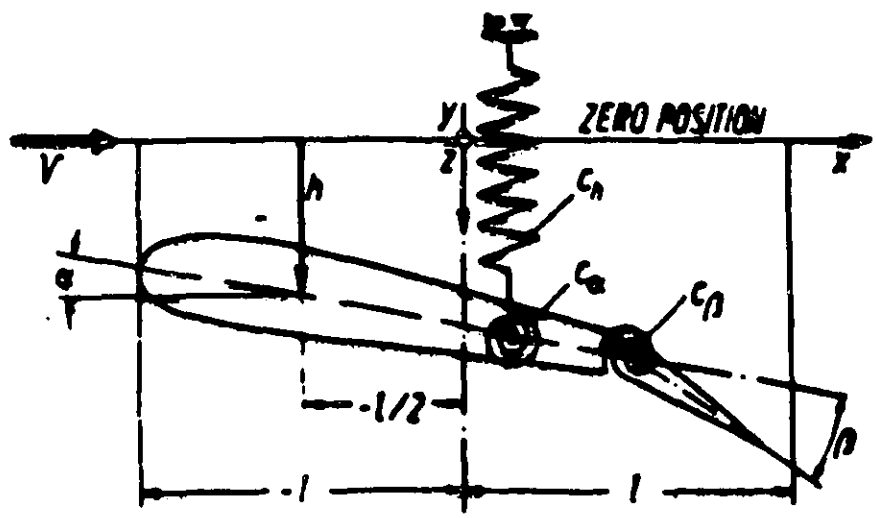

Figure 1.2

Example aeroelastic system with three degrees-of-freedom

Chapter 2

Equations of Motion of the Wing

In this chapter, the aeroelastic equations of motion for the wing are derived. The *direct* equations of motion are constructed from a finite-element description of the wing. These direct equations of motion are expressed in terms of the grid point displacements (translations and rotations). The direct equations are then transformed into *modal* equations in which modal amplitudes are used as (generalised) coordinates. The equations of motion in modal form will be used in the following chapters.

This chapter rigourously outlines the transformation rules between the direct and the modal form of the equations of motion, for further use in Chapters 3 and 4.

2.1 Finite-Element Method

NASTRAN was used for the finite-element structural analysis of the wing.

In a finite-element model, a structure is modelled as being composed of elementary building blocks. Examples of blocks are beams, rods, shells, membranes, hinges .... Building blocks are interconnected at grid points. Every grid point initially has six degrees-of-freedom of motion: three translational and three rotational. Relationships exist between the degrees-of-freedom of different grid points connected by a structural element, and forces and moments applied to the grid points. These relationships depend on the type of structural element. The relationships are algebraic equations for a static analysis or time differential equations for a dynamic analysis. Different types of structural elements connect different numbers of grid points. New types of building blocks can be introduced or constructed from basic elements provided one knows the relationship which the building block imposes on the degrees-of-freedom of the gridpoints it connects.

In addition, boundary conditions constrain the degrees-of-freedom at boundary grid points. The finite-element method is, in general, a numerical method to solve differential equations with given boundary conditions (Boundary Value Problem). By modelling a flexible structure as a composition of elementary blocks, partial differential equations of motion for a continuous structure are discretised and reduced to a set of ordinary time differential equations. The infinite number of degrees-of-freedom of the continuous structure is reduced to a finite number of degrees-of-freedom for the grid points.

Reference [5] provides a comprehensible description of the finite-element method the way it is implemented in NASTRAN. It covers all the structural elements, their use, and the relationships which they impose on the degrees-of-freedom of the grid points they connect. It also explains very clearly how matrices are organised and manipulated in order to eliminate constraints and internal forces (due to the constraints), and build the equations of motion for the degrees-of-freedom of the system.

2.2 Finite-Element Model of the Wing

A finite-element model of the wing consists of a map of the grid points on the wing. Each number corresponds to a grid point identification number. The main elements which connect grid points are elastic beam elements, which together span the two-dimensional surface of the wing. Other elements are rigid connections, hinges, ... The wing inertia is modeled as concentrated masses attached to grid points. An existing structural finite-element model of the wing was employed in this analysis.

The linear wing-fold hinge stiffness value may be modified by editing its value in the above input file to NASTRAN.

One particular wing configuration was used for all calculations in this thesis, corresponding to the antisymmetric modes of the aircraft.

Only one of the two wings is represented in the finite-element model. By selecting the boundary conditions of the wing at the aircraft centerline, one can represent either a symmetric motion or an antisymmetric motion of both wings, seen from the aircraft centerline. The antisymmetric modes were sought in this analysis.

When the wing is not constrained from moving (translating or rotating) as a whole (e.g. the antisymmetric model of the wing can not be constrained from rotating around the aircraft centerline), one or several rigid-body modes will be found. A rigid-body mode represents a motion of the body as a whole, without structural deformation, and has a zero eigenfrequency. For the analyses of oscillatory wing motion in the thesis, a rigid-body mode can be treated as any wing deformation mode, if the rigid-body modal stiffness is set equal to zero. When undamped, a rigid-body mode moves in opposition with its oscillatory forcing function.

NASTRAN execution commands are provided to construct the modal equations of motion of the wing. The modal equations are obtained from the direct equations of motion

through the transformation which is given in the following sections. For calculations used in Chapter 4, it was also important to explicitly obtain the mass and stiffness matrices in the *direct* equations of motion. NASTRAN can be requested to provide the direct mass and stiffness matrices.

2.3 Modal Equations of Motion

In this section, the transformation between the direct and the modal equations of motion is explained, as it is the basis of all further calculations in this thesis.

2.3.1 Modal Transformation

A finite-element analysis of the wing provides the equations of motion for the vector $\{u_a\}$ of the degrees-of-freedom at the grid points

$$[M_{aa}].\{\ddot{u}_a(t)\} + [K_{aa}].\{u_a(t)\} = \{F_a(t)\}. \tag{2.1}$$

These equations are called the *direct* equations of motion. Matrices $[M_{aa}]$ and $[K_{aa}]$ are both symmetric matrices.

We consider the homogeneous equations

$$[M_{aa}].\{\ddot{u}_a\} + [K_{aa}].\{u_a\} = \{0\},$$

often written under the form

$$\{\ddot{u}_a\} + [W_{aa}].\{u_a\} = \{0\}.$$

where $[W_{aa}] = [M_{aa}]^{-1}.[K_{aa}]$. Searching for oscillatory solutions

$$\{u_a(t)\} = \{U_a\}.e^{i\omega t}, \tag{2.2}$$

where $\{U_a\}$ now is a time independent (possibly complex) vector representing the shape of oscillation, we must satisfy

$$-\omega^2.\{U_a\} + [W_{aa}].\{U_a\} = \{0\},$$

or, setting $\omega^2 = \lambda$

$$(\lambda.[I] - [W_{aa}]).\{U_a\} = \{0\}.$$

This is an algebraic eigenvalue problem. We can find the eigenvalues $\lambda_1, \lambda_2, \ldots, \lambda_n$, and the corresponding natural frequencies of oscillation are given by $\omega_i = (\lambda_i)^{\frac{1}{2}}$. Eigenvectors $\{\phi\}_i$ are found by solving equation

$$[W_{aa}].\{\phi\}_i = \lambda_i.\{\phi\}_i. \tag{2.3}$$

We will further assume that all the eigenvalues are distinct. Then, one can easily prove the following orthogonality relations for the eigenvectors

$$\{\phi\}_i^T.[M_{aa}].\{\phi\}_j = 0 \quad for \quad i \neq j, \tag{2.4}$$

$$\{\phi\}_i^T.[K_{aa}].\{\phi\}_j = 0 \quad for \quad i \neq j. \tag{2.5}$$

These above expressions are referred to as *weighted* orthogonality relations. It is important to realise that *simple* orthogonality, i.e.

$$\{\phi\}_i^T.\{\phi\}_j = 0,$$

is not, in general, satisfied. The latter will only be guaranteed if $[W_{aa}]$ is a symmetric matrix.

We can now construct the modal matrix, having as its columns the n eigenvectors.

$$[\Phi] = [\{\phi\}_1 \mid \{\phi\}_2 \mid \ldots \mid \{\phi\}_n].$$

Equation (2.3) can now be written as

$$[W_{aa}].[\Phi] = [\Phi].[\lambda],$$

hence

$$[\lambda] = [\Phi]^{-1}.[W_{aa}].[\Phi]. \tag{2.6}$$

Based on the orthogonality relations, an elegant method exists for inverting the modal matrix[1]. From equations (2.4) and (2.5) we find

$$[M] = [\Phi]^T.[M_{aa}].[\Phi], \tag{2.7}$$

[1] On calculating $[\Phi]^{-1}$.

$$[K] = [\Phi]^T.[K_{aa}].[\Phi]. \tag{2.8}$$

The three matrices $[M], [K]$, and $[\lambda]$ which we introduced are all diagonal, with as their diagonal elements modal masses, modal stiffnesses and eigenvalues respectively. The following relation holds

$$\lambda_i = \frac{K_i}{M_i}.$$

Matrix $[\Phi]$ can be seen as a coordinate transformation matrix where

$$\{u_a(t)\} = [\Phi].\{A(t)\}. \tag{2.9}$$

The new coordinates $A_1, \ldots, A_n$ are called *normal* or *principal coordinates*, or *modal amplitudes.*

2.3.2 Modal Amplitudes

Equation (2.9) provides a meaning for the modal amplitudes. As we have assumed distinct eigenvalues, eigenmodes are independent vectors that span the n-space. Any vector $\{u_a\}$ of grid point displacements can therefore be written as a linear combination of eigenmodes. The coefficients in this linear combination are precisely the principal coordinates or modal amplitudes

$$\{u_a\} = \sum_{i=1}^{n} A_i.\{\phi\}_i. \tag{2.10}$$

As *simple* orthogonality of eigenvectors is not guaranteed: $[\Phi]^{-1} \neq [\Phi]^T$. Still, a computationally interesting way of calculating $[\Phi]^{-1}$ exists, and is given by

$$[M] = [\Phi]^T.[M_{aa}].[\Phi]$$

$$[M]^{-1}.[M] = [I] = [M]^{-1}.[\Phi]^T.[M_{aa}].[\Phi]$$

Hence

$$[\Phi]^{-1} = [M]^{-1}.[\Phi]^T.[M_{aa}]$$

As a diagonal matrix, $[M]$ can easily be inverted.

2.3.3 Modal Equations, Modal Forces

The equations of motion (2.1), rewritten in the new coordinate system, become[2]

$$[M_{aa}].[\Phi].\{\ddot{A}(t)\} + [K_{aa}].[\Phi].\{A(t)\} = \{F_a\}.$$

Premultiplying by $[\Phi]^T$ yields the modal equations of motion

$$[M].\{\ddot{A}(t)\} + [K].\{A(t)\} = \{F(t)\}, \tag{2.11}$$

where

$$\{F(t)\} = [\Phi]^T.\{F_a(t)\},$$

is the vector of *generalised modal forces.* The meaning of the generalised forces is again apparant. The i-th generalised force is obtained as the inner product of the two vectors $\{\phi\}_i$ and $\{F_a\}$.

2.3.4 Damping

In the above modal equations, structural damping has not been introduced. Nevertheless, damping is always present. If the damping mechanism of each individual element in the finite-element model is well understood, a (direct or modal) damping matrix could be constructed in much the same way as the stiffness and mass matrices.

Unfortunately, the various contributions to structural damping are not well understood. The damping matrix cannot be accurately constructed directly from a finite-element analysis. Instead, it is common to use measured values for the damping (obtained from ground vibration tests) and to form the damping matrix from these experimental data.

[2]Of physical interest is only the *mode shape*, not the *norm* of vectors $\{\phi\}_i$. The equations of motion in principal coordinates do not depend on the norm of the eigenvectors, although modal masses, stiffnesses and forces individually do.

Introducing a modal damping matrix $[D]$, the modal equations with damping become

$$[M].\{\ddot{A}(t)\} + [D].\{\dot{A}(t)\} + [K].\{A(t)\} = \{F(t)\}. \tag{2.12}$$

Matrix $[D]$ is assumed diagonal. Its diagonal elements represent *modal* damping values.

2.3.5 Lagrangian Approach

An alternative formulation of the wing dynamics is based on the energy approach. Lagrange's equations of motion are given by

$$\frac{d}{dt}(\frac{\partial T}{\partial \dot{q}_i}) - \frac{\partial T}{\partial q_i} + \frac{\partial V}{\partial q_i} = Q_i \quad i = 1 \ldots n, \tag{2.13}$$

where

T is the kinetic energy of the system (in a motion which satisfies the system constraints),

V is the potential energy stored in the system in motion,

q_i is a set of independent generalised coordinates, and

Q_i is the set of corresponding non-conservative forces.

At each instant in time during motion, expressions for the kinetic and potential energy are

$$T = \frac{1}{2}.\{\dot{u}_a\}^T.[M_{aa}].\{\dot{u}_a\}, \tag{2.14}$$

$$V = \frac{1}{2}.\{u_a\}^T.[K_{aa}].\{u_a\}. \tag{2.15}$$

Introducing the previously defined modal amplitudes as a new set of generalised coordinates, and using weighted orthogonality of eigenmodes, the expression for the kinetic energy becomes

$$T = \frac{1}{2}.\{\sum_{i=1}^{n} \dot{A}_i\{\phi\}_i^T\}.[M_{aa}].\{\sum_{j=1}^{n} \dot{A}_j\{\phi\}_j^T\},$$

$$T = \frac{1}{2} \cdot \sum_i \sum_j \dot{A}_i \dot{A}_j \{\phi_i^T\} . [M_{aa}] . \{\phi\}_j^T,$$

$$T = \frac{1}{2} \sum_{i=1}^{n} M_i \dot{A}_i^2. \tag{2.16}$$

Similarly, one obtains for the potential energy

$$V = \frac{1}{2} \sum_{i=1}^{n} K_i \dot{A}_i^2. \tag{2.17}$$

Using the modal amplitudes as the set of generalised coordinates, and expressions (2.16) and (2.17) for the kinetic and potential energy, Lagrange's equations yield the set of decoupled equations of motion (2.11) obtained previously.

2.4 Forcing Terms

In the following chapters, the modal equations (2.12) are used. They will only differ in the forcing terms. These forcing terms are introduced in two steps

- in Chapter 3, modal aerodynamic forces are introduced. These are aerodynamic forces which are induced by structural vibrations. Introduction of aerodynamic forces yields the aeroelastic equations of motion of the wing in interaction with the flow around the wing. Flutter analysis is performed by analysing the stability of the aeroelastic equations of motion.
- in Chapter 4, additional forces due to aileron oscillations externally imposed during flight testing, are considered.

Chapter 3

Flutter Analysis

To illustrate flutter analysis results, several flutter analyses are performed. Different values of the wing-fold hinge stiffness are assumed. A standard flutter analysis package was used. Flutter analysis results are compared to [4].

Starting from the modal equations of motion, derived in the previous chapter, and by introducing induced aerodynamic forces, the complete aeroelastic equations of motion are obtained. The flutter analysis then consists of an eigenvalue analysis of the homogeneous set of equations.

3.1 Flutter Equations

The modal equations of motion of the wing were derived in Chapter 2:

$$[M].\{\ddot{A}\} + [D].\{\dot{A}\} + [K].\{A\} = \{F\}.$$

Both the mass matrix $[M]$ and the stiffness matrix $[K]$ are diagonal, as the equations are expressed in terms of modal amplitudes, also called *principal coordinates.* The damping matrix $[D]$ was also introduced as a diagonal matrix. Vector $\{F\}$ is the vector of *generalised modal forces.*

For flutter analysis, induced aerodynamic forces due to wing vibrations are introduced

$$\{F\} = \{F_{aero}\}.$$

In flight, wing vibrations modify the flow over the wing, and therefore the aerodynamic forces on the wing. For small *oscillatory* motion of the wing, linearized induced aerodynamic forces can be expressed as

$$\{F_{aero}(t)\} = \frac{1}{2}\rho V^2.[Q_r].\{A(t)\} + \frac{1}{2}\rho V^2.[Q_i].\{\dot{A}(t)\},$$

where the dependence on dynamic pressure is made explicit. Matrices $[Q_r]$ and $[Q_i]$ are fully populated matrices. They express the aerodynamic forces induced by an oscillation in each of the modeshapes on all other modeshapes. The method by which above matrices of induced aerodynamic forces are calculated is introduced in Appendix 1. It is described in detail in [1]. The aerodynamic forces essentially depend on the mode shapes, the modal frequency, and flow parameters as the dynamic pressure and the Mach number.

The equations of motion then become

$$[M].\{\ddot{A}\} + (-\frac{1}{2}\rho V^2.[Q_i] + [D]).\{\dot{A}\} + (-\frac{1}{2}\rho V^2.[Q_r] + [K]).\{A\} = \{0\}. \qquad (3.1)$$

3.2 Flutter Analysis Methodology

A flutter analysis of the equations of motion (3.1) consists of a stability analysis of the system of equations, for different values of flight parameters. An explanation of flutter analysis methods was given in Chapter 1. The flutter analysis method outlined in Chapter 1 can indeed be applied to equation (3.1) which is of the form of equation (1.2).

The matrices $[Q_r]$ and $[Q_i]$ of induced aerodynamic forces depend on the frequency of oscillation of the wing. As explained in Chapter 1, flutter analysis therefore requires an iterative solution process. The iterative method used is known as the P-k method.

The order of the matrices in the aeroelastic equations is equal to the number of degrees of freedom in the finite-element wing model, or approximately 150 for the model used. This is also equal to the number of structural modes of vibration of the wing.

In order to reduce the computational expense of the iterative solution process to practical limits, the order of the equations is reduced by taking into account only a number m (typically 25) of modes. The reduced system of equations of motion is obtained from (3.1) by simply considering the first m modal amplitudes. The first modal amplitudes correspond to the lowest-frequency modes. Because the matrices $[Q_i]$ and $[Q_r]$ are fully populated, it is an approximation to consider only the first m equations.

Nevertheless, a reduction of the order of the equations is considered to provide a good approximation of the exact solution (of a set of equations which is itself an approximate model of the wing structure), as

- *modal* equations of motion are used;
- the lowest frequency modes are retained. They tend to have larger modal amplitudes in a 'natural' vibration of the wing than higher frequency modes;
- any mode beyond the m-th (with m reasonably large) has a 'complicated' mode-

shape, and hence a 'less accurate' influence on the air flow. It will likely 'escape' from coalescence with another mode.

3.3 Flutter Analysis Results

A standard flutter analysis program was used, including

- calculation of matrices of induced aerodynamic forces. Mode shapes and modal frequencies are input.
- flutter analysis, from the aeroelastic equations of motion.

One particular wing was analysed, as explained in Chapter 2. 25 modes are retained for the eigenvalue analysis. The P-k method is used. The flutter analysis is repeated for several values of the wing-fold hinge equivalent stiffness.

Figures 3.1 and 3.2 show the frequency and damping curves for the five lowest-frequency modes, and a nominal wing-fold hinge stiffness. This analysis represents a generic analysis of an aircraft, and thus no numerical values are presented. Flutter occurs at the airspeed where damping of one of the modes becomes negative. A flutter characteristic is also the near-coalescence of frequency for two modes. These two modes are highlighted in Figure 3.1. These are the modes which contribute to the flutter mechanism. The structural modeshapes for these two modes are a bending mode of the wing (all vertical displacements around the wing-tip are in the same direction), and a torsion of the wing outboard.

Varying the wing-fold hinge stiffness had no important influence on the low-frequency modes (modal stiffness and mass, mode shape), except for one mode. This mode is precisely the outer-wing bending mode that contributes to the flutter mechanism. The wing-fold hinge will therefore have an influence on flutter velocity. Figures 3.3 and 3.4 show

the frequency and damping curves for the fluttering modes, for different values of the (equivalent) wing-fold hinge stiffness.

The flight velocity at which flutter occurs increases slightly as the equivalent wing-fold hinge stiffness decreases. Figure 3.5 shows the influence of further reducing the wing-fold hinge stiffness. The wing outboard bending mode frequency drops and coalescence with the uninfluenced torsional mode is deferred to higher airspeeds. The plot of modal damping (not available) showed no unstable mode for the lower wing-fold hinge stiffness.

3.4 Comparison with Lee and Tron

Lee and Tron [4] provide a detailed and extensive study of the influence of the wing-fold hinge, among other nonlinearities, on the wing flutter behaviour. The study in [4] goes far beyond the extent and purpose of this chapter.

Nevertheless, the conclusions from section 3.3 do correspond to influences found in [4]. [4] (fig.8) shows a similar increase in flutter airspeed with reduced wing-fold hinge stiffness. When the wing-fold hinge stiffness is sufficiently reduced, flutter disappears.

It is shown in [4] that, at even lower wing-fold hinge stiffness values, flutter then reappears as a coalescence of a different set of modeshapes, in a limit cycle oscillation typical of nonlinear systems.

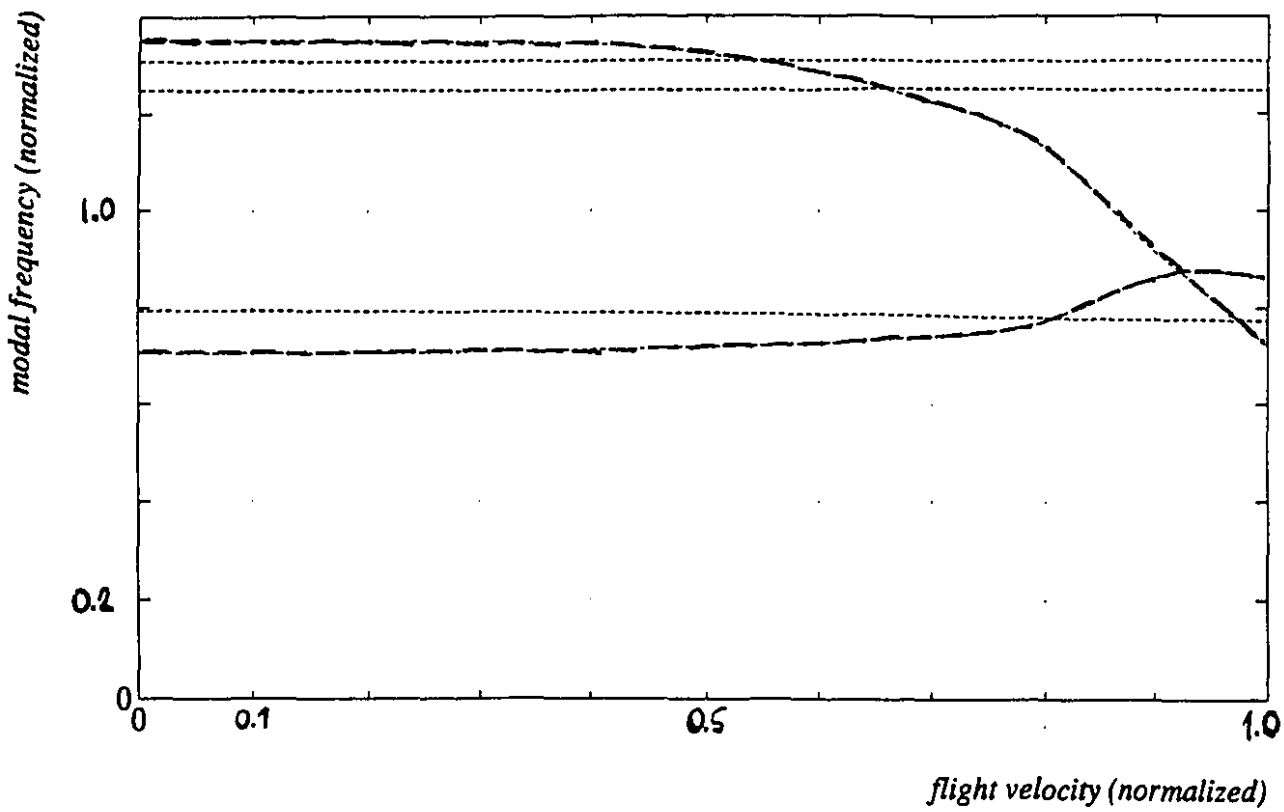

Figure 3.1

Normalized modal frequency versus normalized flight velocity, for five lowest-frequency modes; nominal wing fold hinge stiffness.

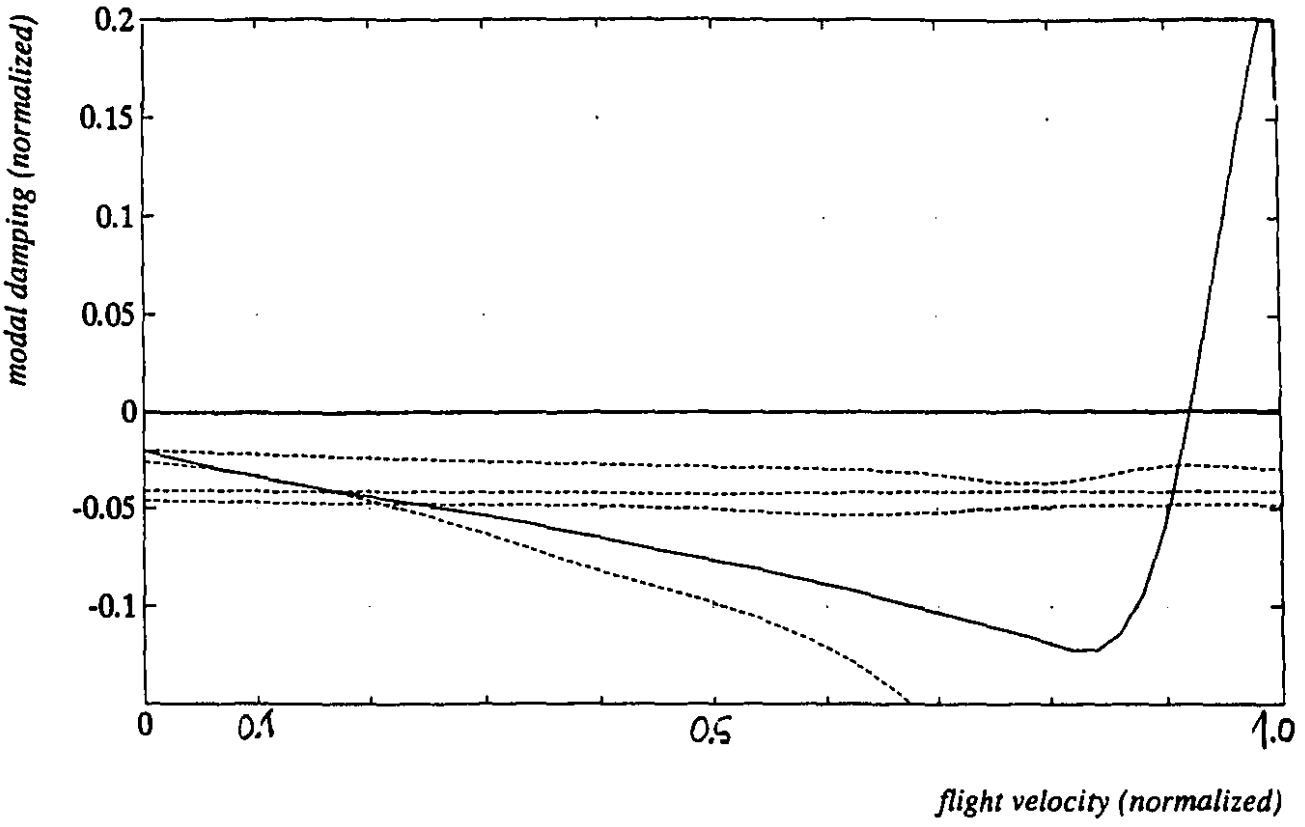

Figure 3.2

Normalized modal damping versus normalized flight velocity, for five lowest-frequency modes; nominal wing-fold hinge stiffness.

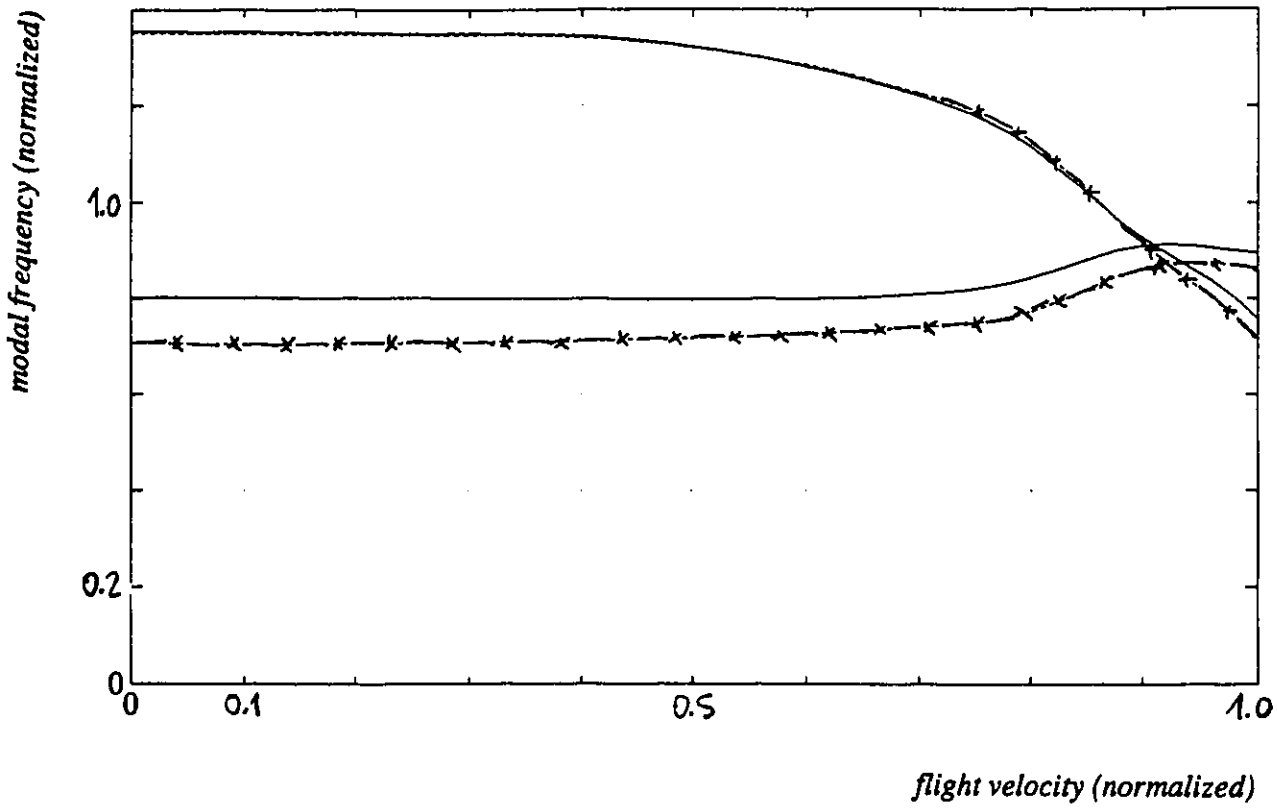

Figure 3.3

Normalized modal frequency versus normalized flight velocity, for two fluttering modes.
——————— : nominal wing fold hinge stiffness
—X—X— : 80% of the nominal wing-fold hinge stiffness

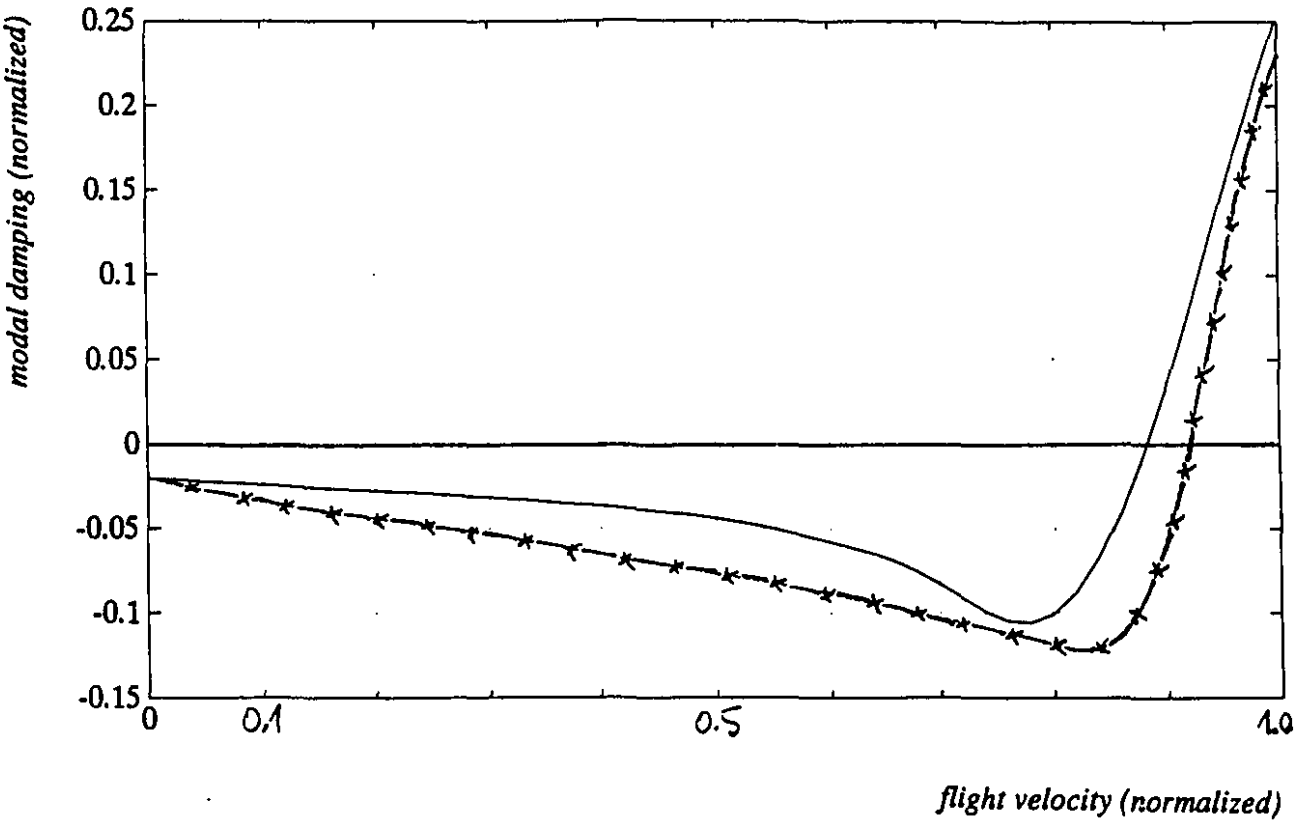

Figure 3.4

Normalized modal damping versus normalized flight velocity, for the unstable mode.
——————— : nominal wing fold hinge stiffness
——×——×—— : 80% of the nominal wing-fold hinge stiffness

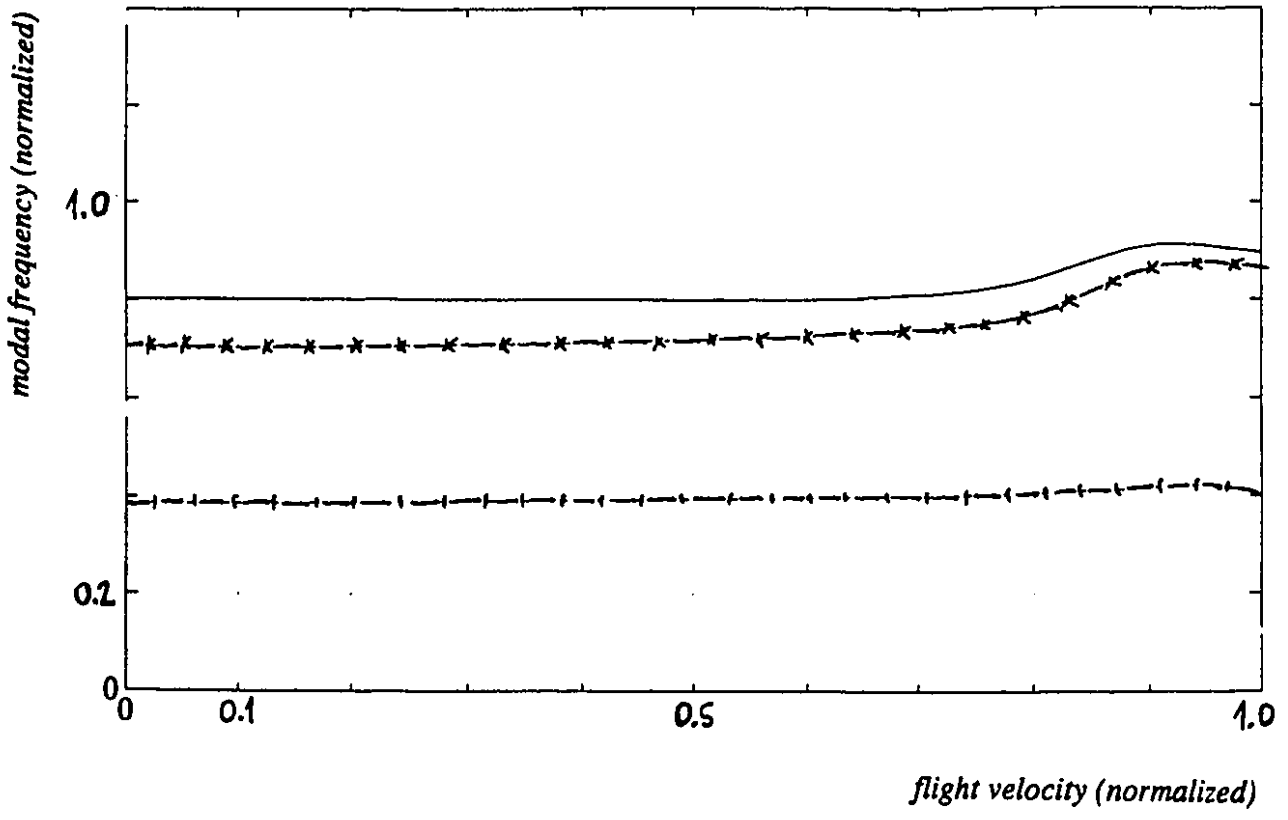

Figure 3.5

Normalized modal frequency versus normalized flight velocity, for the outboard bending mode.
——————— : nominal wing fold hinge stiffness
——×——×—— : 80% of the nominal wing-fold hinge stiffness
——|——|—— : 25% of the nominal wing-fold hinge stiffness

Chapter 4

Forced Aileron Oscillation

Results obtained from theoretical flutter calculations must be verified via flight testing. As part of this testing, it is necessary to provide a known force excitation to the aircraft and then measure the aircraft's response to this excitation. The excitation is provided through forced oscillation of the ailerons. The imposed aileron oscillation causes the complete wing to oscillate due to induced aerodynamic forces. This wing response is measured. Real wing oscillation modes (shape, frequency, damping) are identified by relating the wing response to the imposed excitation. As flight parameters are varied, the aeroelastic modes change. From identified modes, a margin to flutter can be calculated.

For a given aileron oscillation, the wing-fold hinge in particular assumes an oscillatory rotation. An equivalent hinge stiffness corresponds to its oscillation amplitude. The wing behaves as if the wing-fold hinge had a stiffness corresponding to the equivalent linear hinge stiffness. Experimental flutter data should be compared to the theoretical aeroelastic modes calculated for this equivalent stiffness.

In this chapter, we calculate the wing response, resulting equivalent wing-fold hinge stiffness and induced aerodynamic forces for aileron oscillations with different frequencies, amplitudes, and in different flight conditions.

The methodology provided in this chapter is general enough to provide the aerodynamic force on the wing, induced by aileron oscillation, in any form which may be required for the identification of the structural or the aeroelastic modes.

4.1 Equations of Forced Aileron Oscillation Motion

In the equations of motion previously obtained

$$[M].\{\ddot{A}\} + [D].\{\dot{A}\} + [K].\{A\} - \frac{1}{2}\rho V^2.[Q_r].\{A\} - \frac{1}{2}\rho V^2.[Q_i].\{\dot{A}\} = \{F_{ail}\}, \qquad (4.1)$$

we now consider $\{F_{ail}\}$, the forcing terms due to forced aileron oscillation.

As we force the linear system of the equation above with an oscillatory forcing function, the complete system will respond with an oscillatory motion with a frequency equal to the forced aileron oscillation frequency ω_f. By introducing the complex notation

$$\{F_{ail}(t)\} = \{\overline{F}_{ail}\}.e^{j\omega_f t},$$

$$\{A(t)\} = \{\overline{A}\}.e^{j\omega_f t},$$

equation (4.1) transforms into

$$\left((-\omega_f^2[M] + [K] - \frac{1}{2}\rho V^2[Q_r]) + j\omega_f([D] - \frac{1}{2}\rho V^2[Q_i])\right)\{\overline{A}\} = \{\overline{F}_{ail}\}. \qquad (4.2)$$

This system of algebraic equations can be solved for the complex modal amplitudes, if the complex modal forces induced by the aileron oscillation are known.

4.2 Aileron Oscillation Forcing Terms

The forcing terms $\{F_{ail}\}$ can be both structural and aerodynamic.

The ailerons can be freely rotated on the wing. They can be set in any position without statically exerting forces on, or causing deformations of the remaining wing.

The only *structural* forces which are therefore caused on the wing by oscillating the ailerons are dynamic inertia forces caused by the aileron accelerations. These inertia forces, if important, would influence the shape of the wing oscillations, and hence the patterns of induced aerodynamic forces. However, inertia forces are neglected in this chapter. Aileron oscillation inertia forces have been calculated in in other analyses for a range of frequencies of interest to us, and found to be considerably smaller than the aerodynamic forces induced by the aileron oscillation.

The aerodynamic forcing terms express the complex modal forces, induced on each of the natural modes of the wing, by the imposed aileron oscillation mode. They can be calculated by the same method used to calculate the matrices of induced forces in Chapters 2 and 3 (aerodynamic forces of one modeshape on itself and any other modeshape).

In order to apply the computer programs used to calculate the matrices of induced aerodynamic forces in Chapter 3, an artificial wing mode is introduced, representing a pure aileron deflection: appropriate rotations and corresponding displacements are assigned to the grid points on the aileron.

Equation (3.1), when including the added aileron deflection mode, is rewritten as

$$\begin{bmatrix} M_{ff} & 0 \\ \{0\} & [M] \end{bmatrix} \begin{pmatrix} \ddot{A}_f \\ \{\ddot{A}\} \end{pmatrix} + \begin{bmatrix} D_{ff} & 0 \\ \{0\} & [D] \end{bmatrix} \begin{pmatrix} \dot{A}_f \\ \{\dot{A}\} \end{pmatrix} + \begin{bmatrix} K_{ff} & 0 \\ \{0\} & [K] \end{bmatrix} \begin{pmatrix} A_f \\ \{A\} \end{pmatrix}$$
$$- \frac{1}{2}\rho V^2 \left(\begin{bmatrix} Q_{ff_i} & \cdots \\ \{Q_{f_i}\} & [Q_i] \end{bmatrix} \begin{pmatrix} \dot{A}_f \\ \{\dot{A}\} \end{pmatrix} + \begin{bmatrix} Q_{ff_r} & \cdots \\ \{Q_{f_r}\} & [Q_r] \end{bmatrix} \begin{pmatrix} A_f \\ \{A\} \end{pmatrix} \right) \qquad (4.3)$$
$$= \begin{pmatrix} F_{f_{act}} \\ \{0\} \end{pmatrix}$$

(4.3)

The first equation in this set provides the force required to deflect the aileron $F_{f_{ext}}$, but is of no interest to us. For example, it would represent the aileron hinge moment if A_f represented the hinge deflection amplitude. The remaining equations are the modal wing equations for forced aileron oscillation.

After introduction of the complex notation for oscillatory motion with frequency ω_f, they can be rewritten as

$$\left((-\omega_f^2[M] + [K] - \frac{1}{2}\rho V^2[Q_r]) + j\omega_f([D] - \frac{1}{2}\rho V^2[Q_i])\right)\{\overline{A}\} = \{\overline{F}_{ail}\} \qquad (4.4)$$

where

$$\{\overline{F}_{ail}\} = \frac{1}{2}\rho V^2(\{Q_{f_r}\} + j\omega_f\{Q_{f_i}\}).A_f \qquad (4.5)$$

is the vector of complex modal aerodynamic forces on each of the modes, induced by an aileron oscillation of amplitude A_f. The vectors $\{Q_{f_r}\}$ and $\{Q_{f_i}\}$ of aerodynamic forces of the artificial aileron oscillation mode on the natural modes of the wing are obtained by the same numerical method by which matrices of induced aerodynamic forces were obtained (method described in [1]).

Equations (4.4) and (4.5) can be solved for the modal amplitudes $\{\overline{A}\}$, given an aileron deflection of amplitude A_f.

The modal amplitudes determine the response of the wing to the forced aileron oscillation. The aerodynamic forces on the wing are induced both by the external aileron oscillation and by the resulting wing deflection. Due to the assumed linearity of the aerodynamic forces, forces induced by the aileron oscillation can be added to the forces induced by the resulting wing deflections. (Referred to as the 'resulting' wing deflection is the wing deflection caused by the external aileron oscillation; the external aileron oscillation is not part of it.)

4.3 Order Reduction

4.3.1 Approximations

The modal equations of motion are equivalent to the direct equations of motion. A solution of the modal equations, for given initial deflection or given forcing function, provides an exact solution for the finite-element model of the wing. Nevertheless, as the dimension of the system is high (the number of modes is equal to the number of degrees of freedom considered in the finite-elements model; of the order of 150 for our application), solving the system of equations is computationally expensive.

For practical calculations, only a limited number of modes, e.g. 25, is considered in this thesis. The modal amplitudes corresponding to the lowest-frequency structural modes are retained, and further modes are simply neglected in equations (4.1), or (4.4) and (4.5). The solution of the reduced system obtained in this way is an approximation for the correct solution.

Neglecting higher order modes is an approximation because

- the forced aileron oscillation induces aerodynamic forces on all modes, high-order modes as well as low-order modes. It is certainly not the case that this induced force is small for high-order modes.
- high-order modes induce aerodynamic forces on the lower-order modes, as the aerodynamic matrices are fully populated.

Nevertheless, when computation cost imposes an order reduction, retaining the lowest-order modes is a sensible choice as

- the imposed aileron oscillation frequencies are of the order of magnitude of the natural frequencies of the lowest-frequency modes. The modes with higher natural frequency tend to have lower amplitudes in the oscillation of the wing;

- the *natural* modes were chosen as a basis for the modal coordinate transformation, for reasons given in Chapter 1.

The influence of the number of modes which are retained, is assessed in section 4.5.5.

4.3.2 Inverse Coordinate Transformation

For the purpose of modal identification through flight tests, direct forces (acting at grid points instrumented for in-flight mode identification) will be required as a final result, rather than the forces in a modal form.

The inverse coordinate transformation is needed in order to calculate the direct forces, if modal forces are given. Indeed, the formula for transforming an external force $\{F_a\}$ applied to structural grid points, into its modal components $\{F\}$ for the reduced set of modes, is given by

$$\{F\} = [\Phi]^T.\{F_a\}. \tag{4.6}$$

The transformation between direct and modal forces requires particular attention if not all the modes are known. If not all modes, but only a reduced set of the most significant modes are considered in the analysis, we avoid to calculate mode shapes for the remaining modes which are considered not to be significant. NASTRAN is asked to provide only the modeshapes for a number of modes which we consider significant for the analysis. The full matrix $[\Phi]$ is therefore *not* available.

For the i-th modal component, equation (4.6) yields

$$F_i = \{\phi\}_i^T.\{F_a\}.$$

We see that only the i-th mode shape (and not the full $[\Phi]$ matrix) is required in order to obtain the i-th modal force component.

Inversely, trying to obtain the direct force vector $\{F_a\}$ which corresponds to a single modal force F_i is less straightforward. Nevertheless, this is what we need if we want to

calculate the direct force induced on the wing by the imposed aileron oscillation. It is not sufficient to know the i-th mode shape only [1].

Nevertheless, a solution to the problem was found by considering the *weighted* orthogonality relations, e.g.

$$[\Phi]^T.[M_{aa}].[\Phi] = [M].$$

In Chapter 2, it was shown that the above weighted orthogonality relationship can be transformed into

$$([\Phi]^{-1})^T = [M_{aa}]^T.[\Phi].[M]^{-1},$$

The modal mass matrix $[M]$ is a diagonal matrix and therefore easily inverted.
Using

$$\{F_a\} = ([\Phi]^T)^{-1}.\{F\},$$

the equation above is written as

$$\{F_a\} = [M_{aa}]^T.[\Phi].[M]^{-1}.\{F\}.$$

This can be rewritten as [2]

$$\{F_a\} = \sum_i \{F_a\}_i = \sum_i \frac{F_i}{M_i}.[M_{aa}].\{\phi\}_i. \tag{4.7}$$

[1]The reason is that the modal matrix is not orthogonal, i.e. $[\Phi]^{-1} \neq [\Phi]^T$. A geometrical interpretation can be given. As the modal vectors do not form an *orthogonal* set of spanning vectors for the n-space (where n is the number of degrees-of- freedom), *all* the spanning vectors (or modeshapes) are required in order to calculate the projection of a vector on a subspace (the subspace formed by the set of known modeshapes retained in the analysis).

[2]Indeed, as $[M]$ is a diagonal matrix, it is rewritten as

$$\{F_a\} = [M_{aa}]^T.[\Phi].\{\frac{F_i}{M_i}\},$$

which can be interpreted as a sum of the columns of matrix $[M_{aa}]^T.[\Phi]$, multiplied by the corresponding terms of the vector $\{\frac{F_i}{M_i}\}$. As the matrix $[M_{aa}]$ is symmetric, and by the definition of matrix $[\Phi]$, the i-th column of matrix $[M_{aa}]^T.[\Phi]$ is obtained as $[M_{aa}].\{\phi\}_i$.

This equation shows how each single modal force F_i contributes to the vector of direct forces $\{F_a\}$. This contribution is denoted as $\{F_a\}_i$. It also shows that only the modeshape of a particular mode is required to calculate the contribution of that mode, provided that the direct mass matrix is known [3].

Equation (4.7) is used to calculate the direct forces on the wing grid points (components in-phase and out-of-phase w.r.t the aileron forced oscillation) due to aileron oscillation.

Depending on the requirements of the modal identification method, the force on a number of selected grid points may be needed, or a summed force over a region of the wing or the total wing. Further in this chapter, it is assumed that the total aerodynamic force perpendicular to the wing is needed. It is calculated as the sum of the components in the direct force vector $\{F_a\}$ which physically represent a force in that direction.

4.4 Solution Method

Equations (4.4) and (4.5) are solved for the complex modal amplitudes, for a given aileron oscillation amplitude A_f and angular frequency, as well as given flight conditions (equivalent airspeed, Mach number).

The wing-fold hinge rotation due to the imposed aileron oscillation, is obtained in particular. To wing-fold hinge rotation amplitude corresponds an equivalent wing-fold hinge stiffness. On the other hand, the matrices in equations (4.4) depend on this equiva-

[3]Because of the weighted orthogonality relations, the direct mass matrix can be used to invert the modal matrix. It contains sufficient information to avoid calculating all the modeshapes. It contains information equivalent to all of the modeshapes. Similar formulas could be constructed using the direct stiffness matrix.

In a modal analysis session, NASTRAN does not provide the direct mass or stiffness matrix by default. NASTRAN can however be explicitly requested to provide these matrices

lent hinge stiffness. Indeed, the wing-fold hinge is an important structural element in the wing. It influences some of the mode shapes, modal masses and stiffnesses. Also, as the mode shapes change, so do the matrices of induced aerodynamic forces. Therefore, solving equations (4.4) will be an iterative process. Assuming an initial value for the equivalent hinge stiffness, we calculate the wing deflection in response to the aileron oscillation. The wing-fold hinge rotation is obtained from the oscillation of the complete wing. To this hinge deflection corresponds an equivalent stiffness which is a better approximation than the initial guess. This is used in the second iteration step.

In Chapter 1, we emphasised the fact that aerodynamic forces on a mode induced by another mode, depend on the frequency of vibration of this latter mode. This raised problems for flutter analysis, and was the reason for a distinction between different methods for flutter analysis (P vs. P-k). Fortunately, this problem does not occur here. As the complete wing is forced to vibrate with a given angular frequency ω_f, induced aerodynamic forces should be calculated at this forcing frequency.

As structural and aerodynamic calculations depend on the wing-fold hinge stiffness and the reduced frequency, they must be repeated for each new value of these parameters. To limit the expense of calculations, they are performed for several 'hard' values of the parameters, and results for intermediate values are obtained by interpolation.

The steps implemented to solve equations (4.4) and (4.5) are as follows.

1. For different 'hard' wing-fold hinge stiffnesses, calculate the structural data (eigenfrequencies, eigenmodes, modal masses and stiffness).

2. For each of the above sets of eigenmodes, and for each 'hard' value of reduced frequency, calculate the matrices of aerodynamic forces.

3. Choose values for the aileron oscillation amplitude and frequency, and flight parameters. Assume an initial value for the equivalent hinge stiffness.

4. For each of the hard equivalent stiffnesses, interpolate aerodynamic forces to the reduced frequency corresponding to the given aileron frequency.

5. Interpolate modal data to the actual equivalent stiffness. Also interpolate aerodynamic data (those were already interpolated to the correct reduced frequency in step 4) to this equivalent stiffness.

6. Build and solve the system of equations.

7. Extract the hinge oscillation from the resulting wing motion. Calculate the corresponding hinge equivalent stiffness. Take this as the new value for the equivalent stiffness. If this stiffness is equal to the assumed stiffness, go to step 8, otherwise go back to step 5.

8. End.

Once the complex modal amplitudes are obtained, the corresponding induced aerodynamic modal forces are calculated. They are added to the modal forces directly induced by the aileron oscillation mode in order to obtain the total [4] aerodynamic modal forces induced on the wing. Equation (4.7) is used to transform modal forces into direct forces on the wing.

4.5 Results

Complex amplitudes are obtained for typically 25 modes. For each mode shape, the corresponding (complex) grid point deflections can be calculated, and the vector-sum

[4]This total induced aerodynamic force on the wing is calculated in this thesis and shown in the figures of section 4.5. Nevertheless, if the *aeroelastic* modes need to be identified in the flight tests, only the modal forces directly induced by the aileron oscillation should be considered (and not the total induced aerodynamic force which also includes the aerodynamic force induced by the resulting wing deflection). This is seen from Equation 4.2.

taken for all the modes considered.

From the resulting modal amplitudes, the corresponding modal aerodynamic forces can be determined. Using the inverse modal matrix, these can be transformed into direct forces on the wing. This is done in order to calculate the total aerodynamic force (its amplitude and phase) induced via the forced aileron oscillation.

All results are obtained for a Mach number of 0.95. The wing configuration was given in Chapter 2. Different values of the equivalent airspeed and the aileron oscillation amplitude are taken. All results are obtained as functions of the aileron oscillation frequency.

Because of the generic nature of this work the aileron oscillation frequency, as well as all results shown on graphs, are normalized and no numerical values are presented.

4.5.1 Modal Amplitudes

Figure 4.1 shows a typical response of one degree-of-freedom of the wing in several different modes. In particular, the modal contributions to the wing-fold hinge rotation are given, resulting from the forced aileron oscillation. In reality, the response in each of the modes is a complex number, with an amplitude and a phase difference w.r.t the aileron oscillation. In Figure 4.1 only the amplitude of the modal responses is represented. The amplitudes for five flexible modes are shown as functions of the forcing frequency, for one value of the aileron oscillation amplitude, the equivalent airspeed and the Mach number.

In particular, Figure 4.1 gives the modal contributions to the wing-fold hinge rotation for the two modes shown in Chapter 3 to potentially cause flutter. These modes are an outer-wing bending mode, and a wing tip torsional mode.

It is difficult to interpret exactly the shape of these curves, as they are a result of

- the dependence of the generalised forces, hence the system matrices, on the reduced

frequency.

- the dependence of the natural modes, hence the modal matrices and aerodynamic matrices, on the wing-fold hinge stiffness. This hinge stiffness is itself dependent on the total wing-fold hinge deflection obtained by solving the system of equations.

- the poor linear interpolation method used to interpolate between the 'hard' reduced frequencies and the 'hard' equivalent hinge stiffnesses.

- the coupling between modes due to induced aerodynamics. Indeed, the modal mass and stiffness matrices are diagonal, but the matrices of induced aerodynamic forces are highly non-diagonal.

- the aerodynamic modal forcing terms. The imposed aileron oscillation induces aerodynamic forces on each of the modes considered. The magnitude of these forces depends on the modeshapes, and shows important variations from one mode to the other.

The influence of the aerodynamic forces induced by the imposed aileron oscillation is apparant from Figure 4.1:

- from the modeshape of the outer-wing bending mode (Figure 3.5), one understands that the aileron oscillation will induce a high aerodynamic force on this mode. This is reflected in the high amplitude of this mode in Figure 4.1, for all values of the aileron oscillation frequency.

- for certain values of the aileron oscillation frequency, several modes show a clear peak in their response amplitude. This is likely due to the fact that modes are excited around their natural frequency, the modeshapes of which are likely to induce important aerodynamic forces on other modes.

4.5.2 Equivalent Hinge Stiffness and Induced Aerodynamic Force

If the complex sum is made of the modal wing-fold hinge deflections, the amplitude of this sum is the resulting deflection of the wing-fold hinge. The equivalent stiffness is calculated which corresponds to the hinge oscillation amplitude. This stiffness is a better approximation for the exact hinge stiffness, than the initial guess on which the system equations were based. The iterative procedure leading to the equivalent wing-fold hinge stiffness was described in a section 4.4.

As long as the wing-fold hinge deflection is smaller than the hinge deflection due to preloading, the hinge equivalent stiffness is equal to the nominal stiffness. If the hinge oscillation amplitude becomes larger than the preloading deflection, the equivalent hinge stiffness decreases. System equations must be recalculated using the new value of the hinge stiffness.

The iterative procedure converges in most cases. Nevertheless, for some combinations of parameters, the iteration is caught in a limit cycle. Assume that a large initial guess for the equivalent hinge stiffness results in a large hinge oscillation, for the given parameter combination (this may seem contradictory, but it is perfectly possible). With this large oscillation amplitude corresponds a lower equivalent stiffness. In the next iteration step, this lower stiffness may very well result in a low hinge oscillation amplitude, and hence the high equivalent stiffness of the very first guess. Choosing a new starting value for the iteration is often no solution to the problem, as the iteration will diverge to the same limit cycle. A simple way of solving the problem is to divide the interval of equivalent stiffnesses, delimited by the limit cycle, into subintervals of the required accuracy on the stiffness. The system is solved for each of the subintevals. For each resulting hinge rotation, the equivalent hinge stiffness is calculated. The correct initial stiffness is the one which is closest to the equivalent stiffness of the hinge rotation obtained with

this initial stiffness. Although this solution is computationally expensive, it is justified by the fact that few instances of divergence occurred. Choosing a more refined interpolation algorithm between the hard equivalent hinge stiffnesses would improve the convergence of the algorithm and the accuracy of the solution.

Figure 4.2 gives graphs of the wing-fold hinge rotation amplitude versus the aileron oscillation frequency. The three graphs correspond to equivalent airspeeds of V, 1.43V and 1.86V respectively, and a 2 degree aileron oscillation amplitude. Figure 4.3 provides graphs of the equivalent wing-fold hinge stiffness corresponding to the wing-fold hinge oscillation amplitudes from Figure 4.2. Figure 4.4 provides graphs of the total aerodynamic force (perpendicular to the wing) acting on the wing due to forced aileron oscillation and the induced wing oscillatory motion. Only the amplitude of the aerodynamic force is given. Graphs of the phase difference with respect to the inducing aileron oscillation are given in section 4.5.3.

From Figures 4.2 to 4.4, one can conclude that

- to sufficiently high hinge rotations correspond significant dips in equivalent hinge stiffness. If the ailerons are oscillated in flight tests, with an amplitude and at a frequency which give rise to a large hinge rotation amplitude and a decreased wing-fold hinge equivalent stiffness, then the modes identified from these flight test recordings should be compared to the calculated (from the finite- element model) modes at that reduced equivalent hinge stiffness.

- peaks in the total aerodynamic force induced on the wing roughly correspond to peaks in the hinge rotation. They also show on Figure 4.1. As was already mentioned for Figure 4.1, these peaks were likely due to the excitation, at particular aileron oscillation frequencies, of particular modes which induce high aerodynamic forces on other modes. This is confirmed by the peaks in the total wing aerodynamic force on Figure 4.4.

- For an equivalent airspeed of V (and for the given values of the aileron oscillation amplitude, Mach number and wing-fold hinge preload), the equivalent wing-fold hinge stiffness only decreases in one zone of aileron oscillation frequency. Even then, this zone is relatively broad and a stiffness reduction of 20% is seen. The broad basis of the peak can be explained by the fact that the mode which causes the dip (outer-wing bending mode, Figure 4.1), is also the mode which is most sensitive to variations of the equivalent stiffness (this was shown in Chapter 3). For the higher airspeeds of 1.43V and 1.86V, the dips in wing-fold hinge equivalent stiffness occur at a variety of aileron oscillation frequencies, and are more difficult to isolate.

4.5.3 Phase Information of Induced Aerodynamic Force

If the total induced aerodynamic force on the wing is used in modal identification of the wing vibration modes, the phase difference between the aileron oscillation and this aerodynamic force is an important information.

Figure 4.5 shows the variation of the phase angle of the total aerodynamic force, as a function of the aileron oscillation frequency, for a 2 degree aileron oscillation amplitude and 1.43V. The phase angle represents a phase lead of the aerodynamic force with respect to the aileron oscillation.

It is apparant that, for most frequencies, there is a 50 to 100 degrees lag of the aerodynamic force behind the aileron displacement.

Figure 4.5 shows considerable variations in the phase angle. It should however be noted that the graph would appear smoother by appropriately adding or subtracting 360 degrees to/from phase angles.

Similar curves are obtained for other values of aileron oscillation amplitude and equivalent airspeed.

4.5.4 Effect of the Nonlinearity

Figures 4.6 through 4.8 show the wing-fold hinge rotation, the equivalent hinge stiffness and the total induced aerodynamic force for aileron oscillation amplitudes of 1 and 2 degrees respectively, and 1.43V. Nonlinear behaviour clearly appears when the wing-fold hinge oscillates in its nonlinear zone. In Figure 4.6, the nonlinearity gives that the response for 2 degrees aileron oscillation amplitude is not equal to twice the response for an amplitude of 1 degree. The effect is amplified in Figure 4.8.

Figure 4.9 compares the wing-fold hinge rotation curve obtained for the nonlinear wing-fold hinge, with curves which would be obtained if a linear wing-fold hinge were assumed (with a stiffness independent of the wing-fold hinge rotation amplitude). Linear stiffnesses equal to the nominal wing-fold hinge stiffness and 75% of the nominal value were assumed respectively. The three curves of Figure 4.9 assume 2 degrees aileron deflection amplitude and 1.43V.

Figure 4.10 gives the total wing aerodynamic force for the assumptions of Figure 4.9. On Figure 4.9, the response for the nonlinear hinge evolves between the curves corresponding to the linear wing-fold hinge stiffnesses. This was expected, given the variations of the equivalent linear wing-fold hinge stiffnesses for the nonlinear wing-fold hinge, shown on Figure 4.7.

Figure 4.10 shows a peak in the aerodynamic force for the nonlinear hinge (around a 0.4 normalised aileron oscillation frequency) which largely exeeds the corresponding aerodynamic force for the 'enveloping' linear wing-fold hinges. This indicates that the total induced aerodynamic force calculated on the wing is a very sensitive parameter. This sensitivity may limit the usefulness of the total aerodynamic force for modal identification purposes, especially in zones where it varies considerably. Note that the same peak is found on Figure 4.8, where it is even amplified if the aileron oscillation amplitude decreases.

4.5.5 Effect of the Number of Modes

Figure 4.11 through 4.13 show the influence of the number of modes retained in the calculations. A 2 degrees aileron oscillation amplitude and 1.43V are assumed. A linear wing-fold hinge is assumed, with a stiffness equal to the nominal hinge stiffness value.

Figure 4.11 gives curves of the wing-fold hinge deflection amplitude, when 18, 22 and 25 modes respectively are retained in the calculations. Peaks progressively appear in the solution, as an increasing number of modes is retained. The mode identifications added to the peaks in Figure 4.11 indicate the smallest number of modes to retain, for that peak to appear in the solution. Peaks which have an important effect on the results discussed in this thesis, require a surprisingly high number of modes to be retained in the calculations. This is most likely due to aerodynamic forces induced between modes.

Figure 4.12 shows the corresponding aerodynamic forces. No convergence at all seems to occur, even as the number of modes considered for the calculations exceeds 20. This certainly confirms that the *total* induced aerodynamic force is a very sensitive variable. This is understandable as it is the *sum* of aerodynamic forces at all grid points on the wing. Each of the grid point forces is itself obtained as a sum of transformed modal forces. It is likely that induced aerodynamic forces at selected individual grid points are vales which are less sensitive to the number of modes.

Figure 4.13 is more satisfying. The phase of the total aerodynamic force seems to be a stabler variable than the corresponding amplitude.

4.5.6 Effect of the Wing Flexibility

It is interesting to evaluate the influence of the wing flexibility on the results obtained above. In this section, a comparison is made with results which are obtained for pure aileron deflection, assuming no deformation of the wing.

Results for the rigid wing are first obtained by applying the methods of this chapter. The amplitudes of all flexible modes are set to zero. Only the amplitudes of the rigid body modes are different from zero, due to aerodynamic forces induced by the aileron oscillation. These results are then compared to similar results obtained through a more straightforward method referred to as Method 2 in the summary hereafter.

Method 1: Using the Flexible-Wing Model

The method used to calculate the total aerodynamic force on the flexible wing can be applied to a wing which is assumed to be rigid, if the amplitude of the wing deformation modes is made zero.

As explained in section 4.3.2, the contribution from each mode to the direct force vector, is obtained from the corresponding modal force by the following transformation formula:

$$\{F_a\}_i = \frac{F_i}{M_i}[M_{aa}]\{\phi\}_i.$$

The vector of direct aerodynamic forces, for all modal components, is obtained by summing the modal contributions [5]

$$\{F_a\} = \sum_i \{F_a\}_i.$$

As all wing deformation amplitudes are set equal to zero (rigid wing), the modal aerodynamic forces are induced only by the forced aileron oscillation mode, and the rigid-body oscillation modes of the wing.

[5]This sum must be taken over ALL the modes of the wing model, rigid-body modes as well as the flexible modes. This assumption of a rigid wing will influence the values of the modal aerodynamic forces, but not the number of terms in this sum. This follows from the strict mathematical derivations. It can also be understood qualitatively. Indeed, the direct force contribution from any mode acts only on the contributing mass of that particular mode. Contributions of all modes are required to find the direct force acting on the total mass of the wing. The influence of the modal masses is apparant from the transformation formula between the modal and the direct forces.

Although working with the flexible-wing model to calculate the response of a rigid wing is not a recommended method for solving the simple rigid-wing problem, it was a straightforward application of the general method of this chapter.

Method 2: Using the Rigid-Wing Model

A previous method and calculation results for the total aerodynamic force amplitude and phase on the wing (assumed rigid), due to imposed aileron oscillations, were available.

The method used in the previous analysis differs from 'method 1' described above, as it assumes a rigid wing to start with, whereas method 1 obtained the rigidity of the wing by setting deformation amplitudes in a flexible wing model equal to zero.

Induced aerodynamic forces used in this previous analysis are calculated by the same method as the aerodynamic forces used in this thesis, i.e. as *modal* aerodynamic forces. If F_{rigid} is the modal force induced by the aileron oscillation on the rigid-body mode of the wing, then the corresponding *direct* force vector $\{F_a\}$ is *implicitly* given by

$$\{\phi_i\}^T\{F_a\} = F_{rigid}.$$

If all components of the modeshape $\{\phi_i\}$ are equal to 1 (i.e. the rigid-body modeshape is a unit heave), then the left hand side of above equation is equal to the sum of the components of the vector $\{F_a\}$, which is precisely the total aerodynamic force induced on the rigid wing due to the aileron oscillation.

In order to obtain the total aerodynamic force (perpendicular to the wing, and induced by the aileron oscillation) by this method, it was necessary to assume the unit heave wing mode.

However, due to the asymmetric configuration of the wing model used in this thesis, a unit heave rigid-body mode of the wing does not occur (as it would assume the symmetric configuration). Therefore, we believe that the previous method does not calculate the

same 'total aerodynamic force' on the wing, as the one calculated by method 1, as this total force on the wing depends on the rigid-body mode which the wing can assume in its proposed configuration (symmetric versus asymmetric).

If the previous method had assumed a rigid-body mode corresponding to the asymmetric wing configuration, the modal induced force of the aileron oscillation on the rigid-body mode would not have been an exact representation of the total direct aerodynamic force perpendicular to the wing.

Comparison of Results

Figure 4.14 gives the total aerodynamic force on the wing for the flexible wing, as well as for the rigid wing. Rigid wing results are shown obtained using both methods described above (although the values obtained with 'method 2' are not believed to exactly represent the total aerodynamic force). A 2 degrees aileron oscillation amplitude and 1.43V are assumed. The results for the flexible wing assume a linear wing-fold hinge stiffness with the nominal hinge stiffness value. The results of the rigid wing, method 2, are taken from the existing previous analysis (1.43V, M=0.95, values scaled to 2 deg. aileron oscillation, forces on the wing and the aileron panels are added).

Figure 4.15 gives the phase angle (phase lead w.r.t. the aileron motion) of the total aerodynamic force, corresponding to the graphs of Figure 4.14.

Figures 4.14 and 4.15 show discrepancies between the rigid wing results obtained using 'method 1' and 'method 2'. This may be due to the difference in the assumed rigid-body mode. The result for the rigid wing, obtained through 'method 1' should be compared to the results for the flexible wing. From Figure 4.14, it is seen that, at distinct values of the aileron oscillation frequency, significant differences occur between the rigid and the flexible wing. Also, it is seen from Figure 4.15 that the wing flexibility systematically causes a shift of the phase angle of the total aerodynamic force with respect

to the rigid wing assumption.

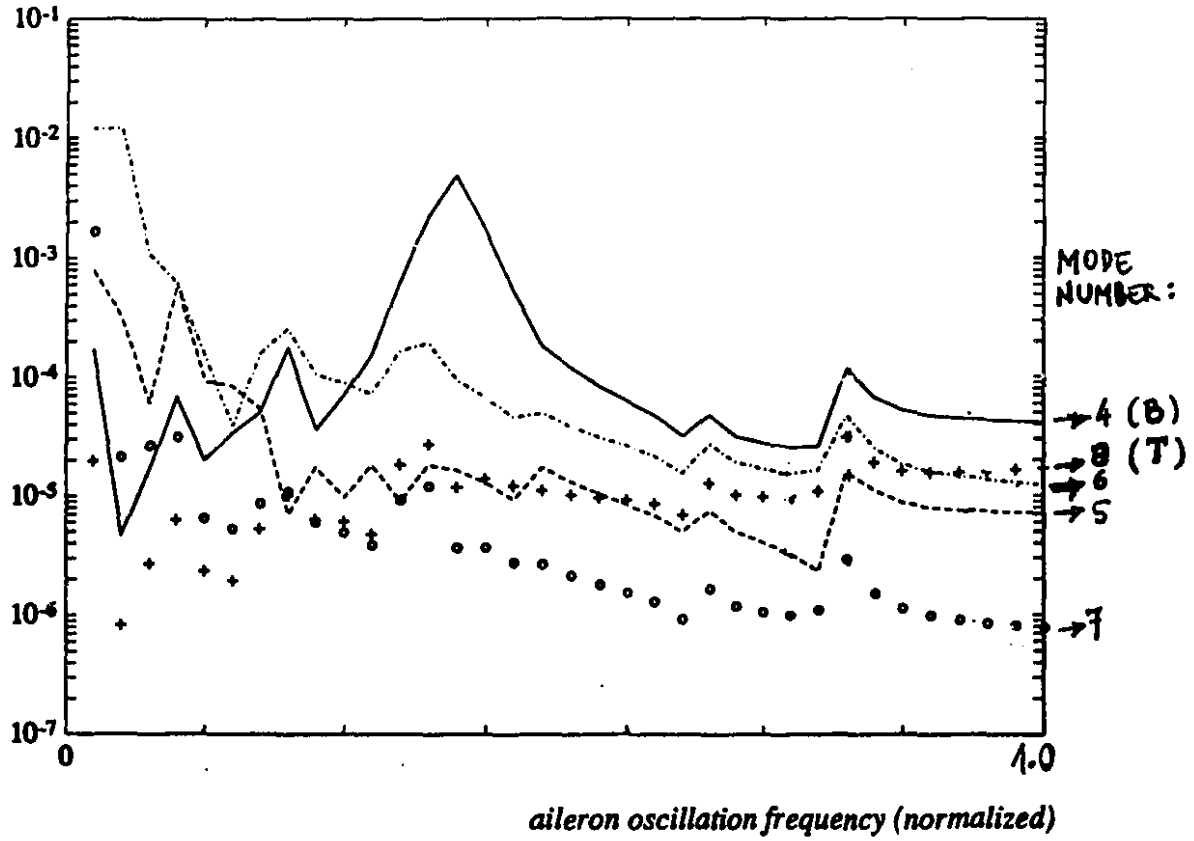

Figure 4.1

Modal contributions to hinge rotation, versus aileron oscillation frequency; for 5 lowest-frequency modes;
B: outer-wing bending mode;
T: wing tip torsion;
B and T are the modes which potentially cause flutter)

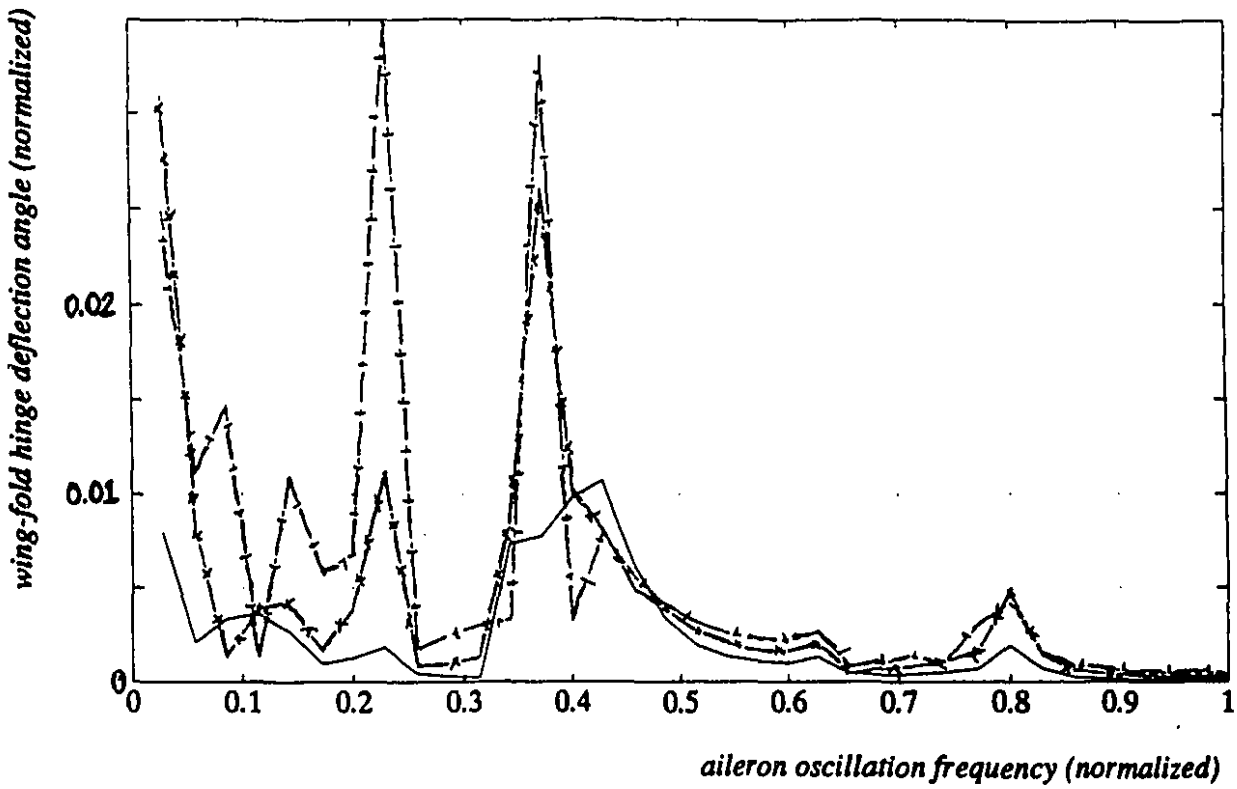

Figure 4.2

Wing-fold hinge rotation amplitude versus aileron oscillation frequency, for 2 degrees aileron oscillation amplitude , at different airspeeds :

——————— *: V*

—X—X— *: 1.43 V*

—|—|— *: 1.86 V*

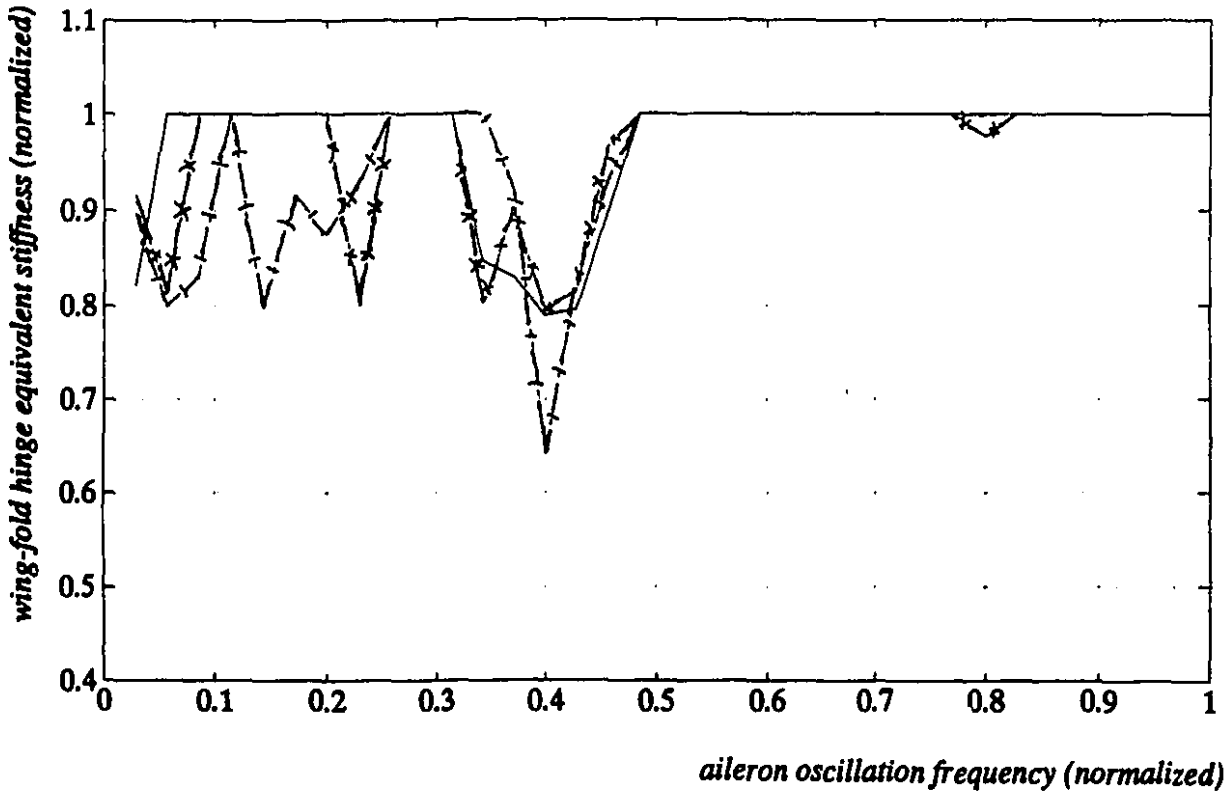

Figure 4.3

Wing-fold hinge equivalent stiffness versus aileron oscillation frequency, for the aileron oscillation amplitude and airspeeds corresponding to Figure 4.2.

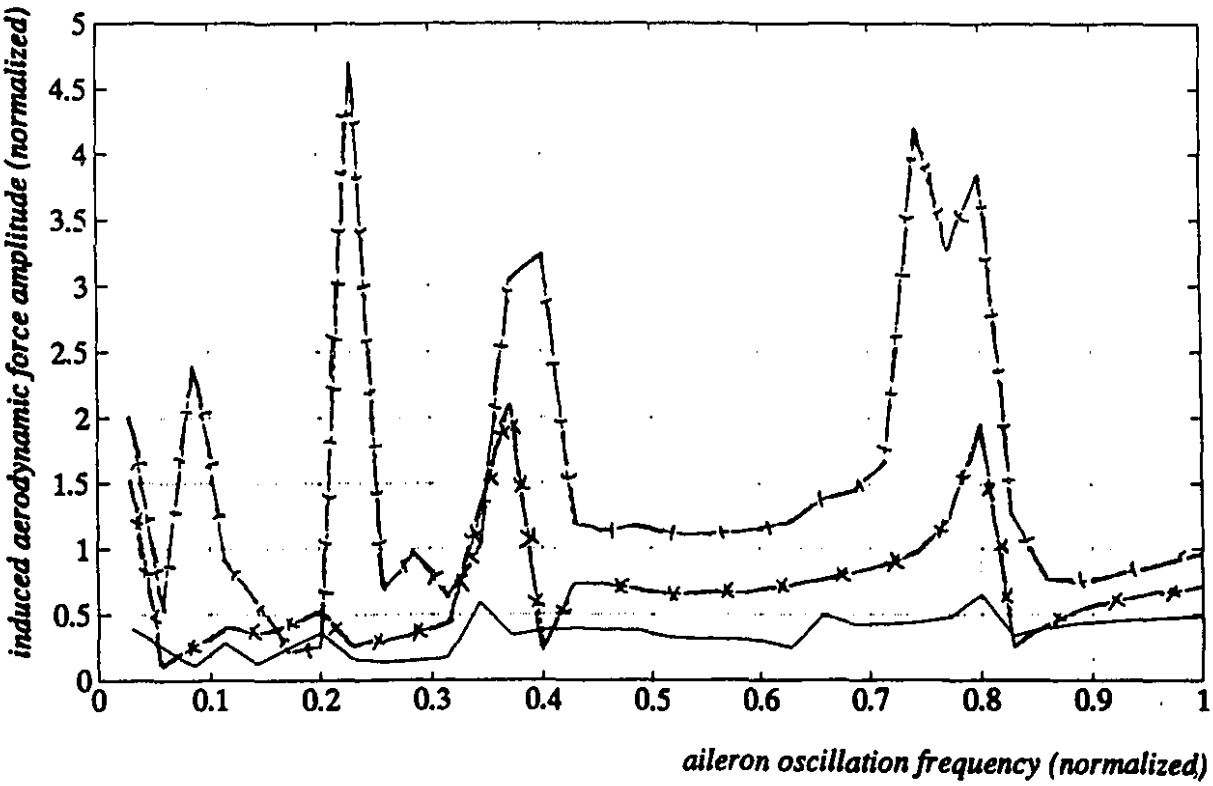

Figure 4.4

Total induced aerodynamic force versus aileron oscillation frequency, for aileron oscillation amplitude and airspeeds corresponding to Figure 4.2

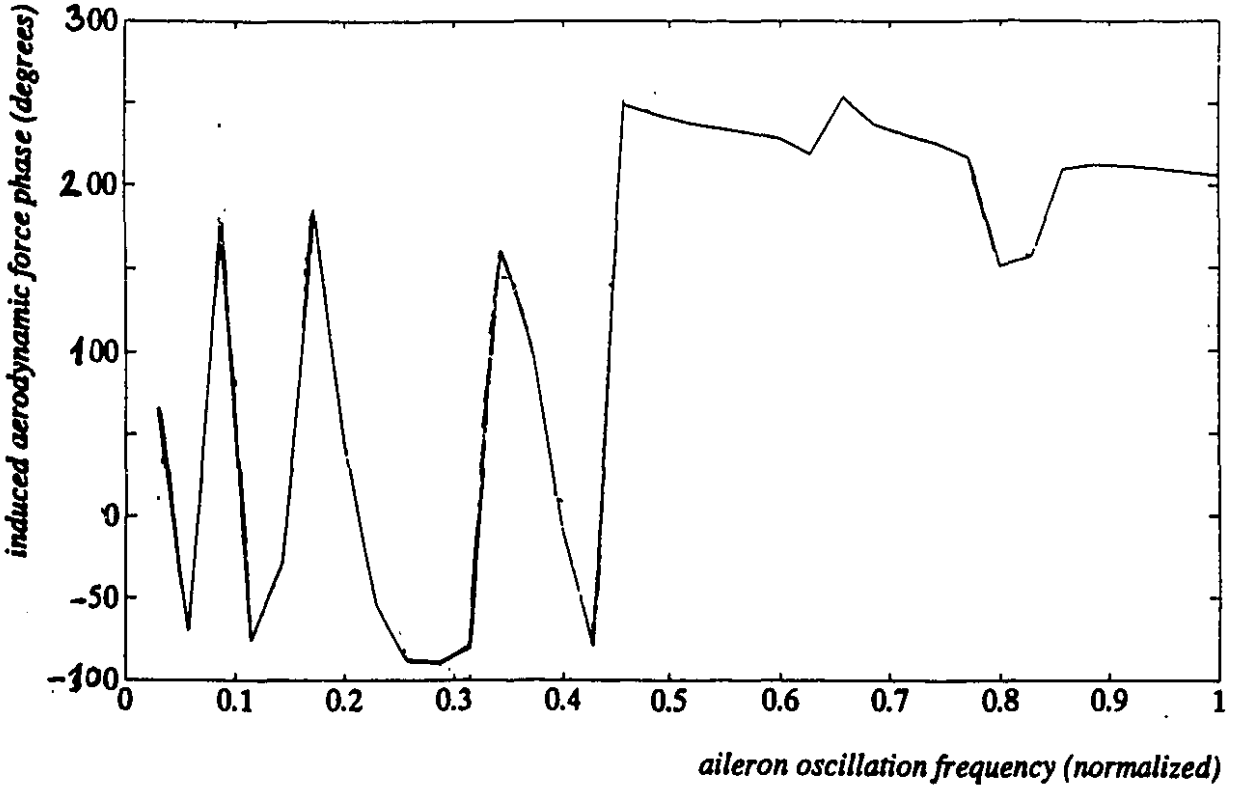

Figure 4.5

Total aerodynamic force phase angle versus aileron oscillation frequency, for 2 degrees aileron oscillation amplitude, and 1.43 V

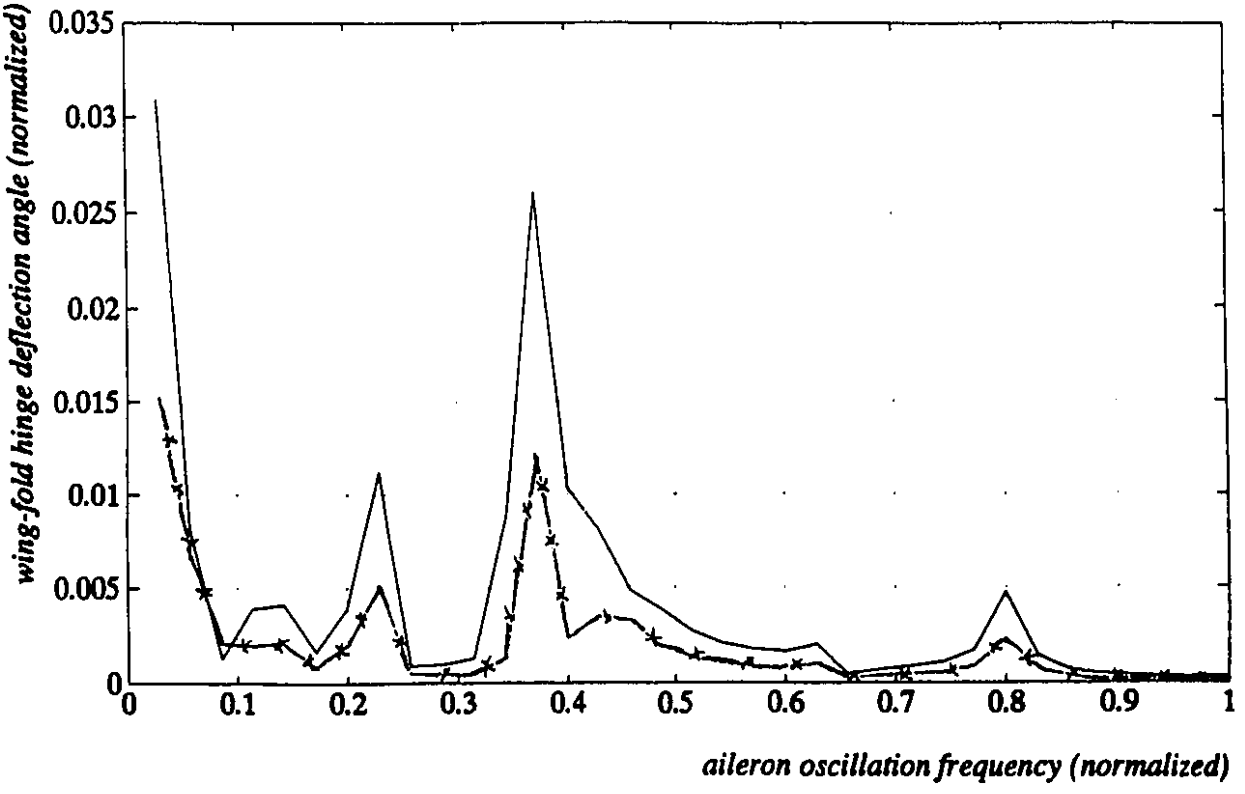

Figure 4.6

Hinge rotation amplitude versus aileron oscillation frequency, for 1.43 V, and aileron oscillation amplitudes of 1, resp. 2 degrees.

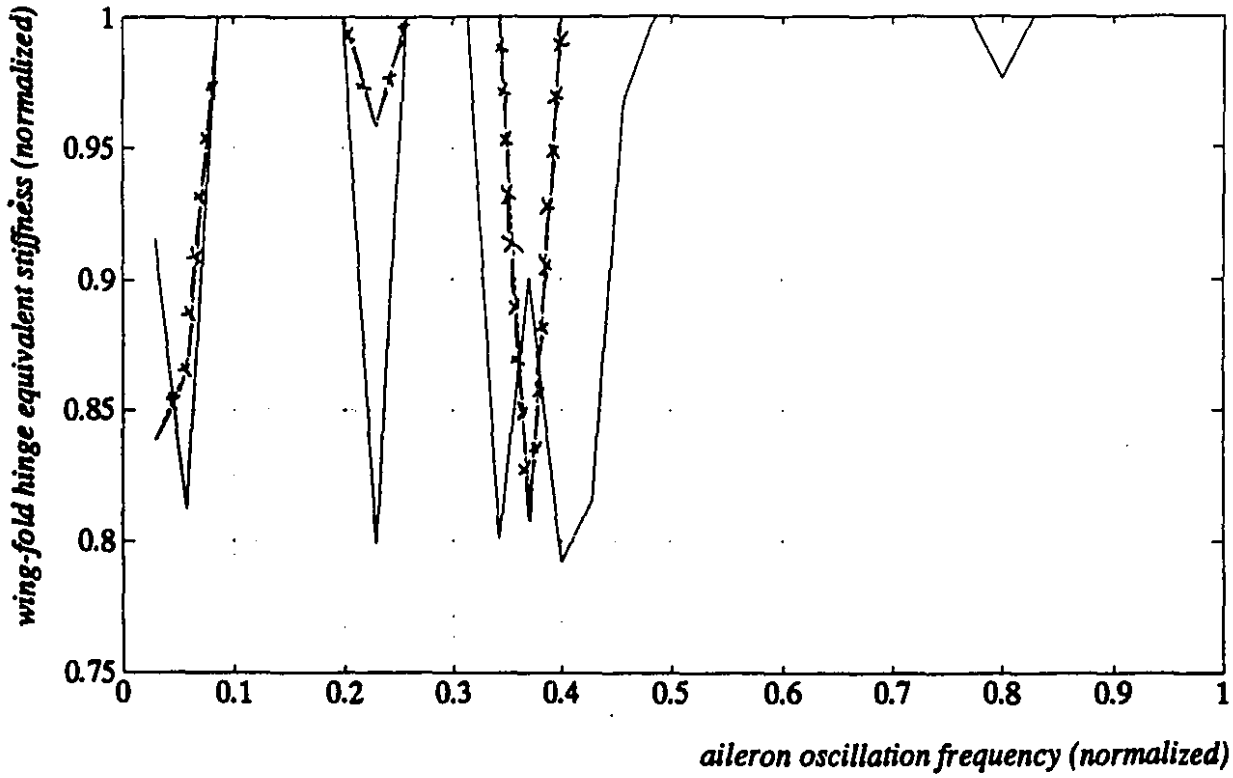

Figure 4.7

Wing-fold hinge equivalent stiffness versus aileron oscillation frequency, for aileron oscillation amplitudes and airspeed corresponding to Figure 4.6

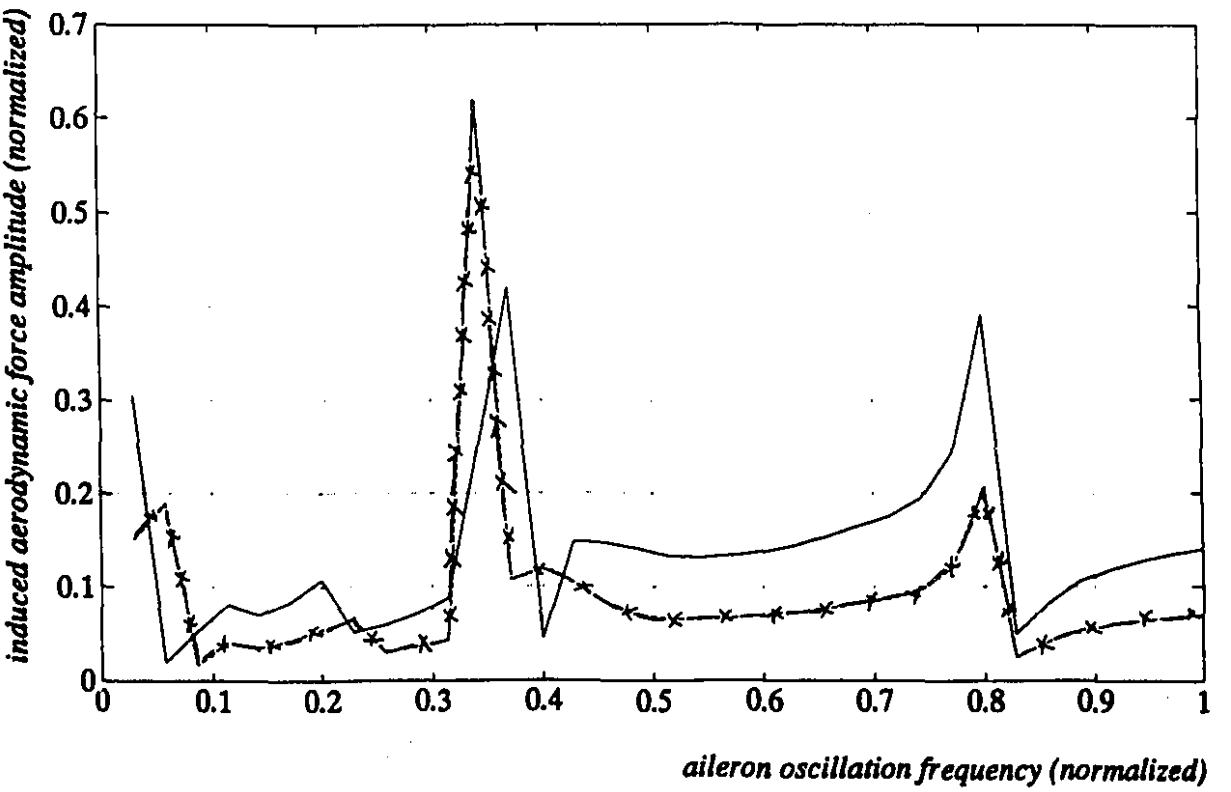

Figure 4.8

Total aerodynamic force versus aileron oscillation frequency, for aileron oscillation amplitudes and airspeed corresponding to Figure 4.6

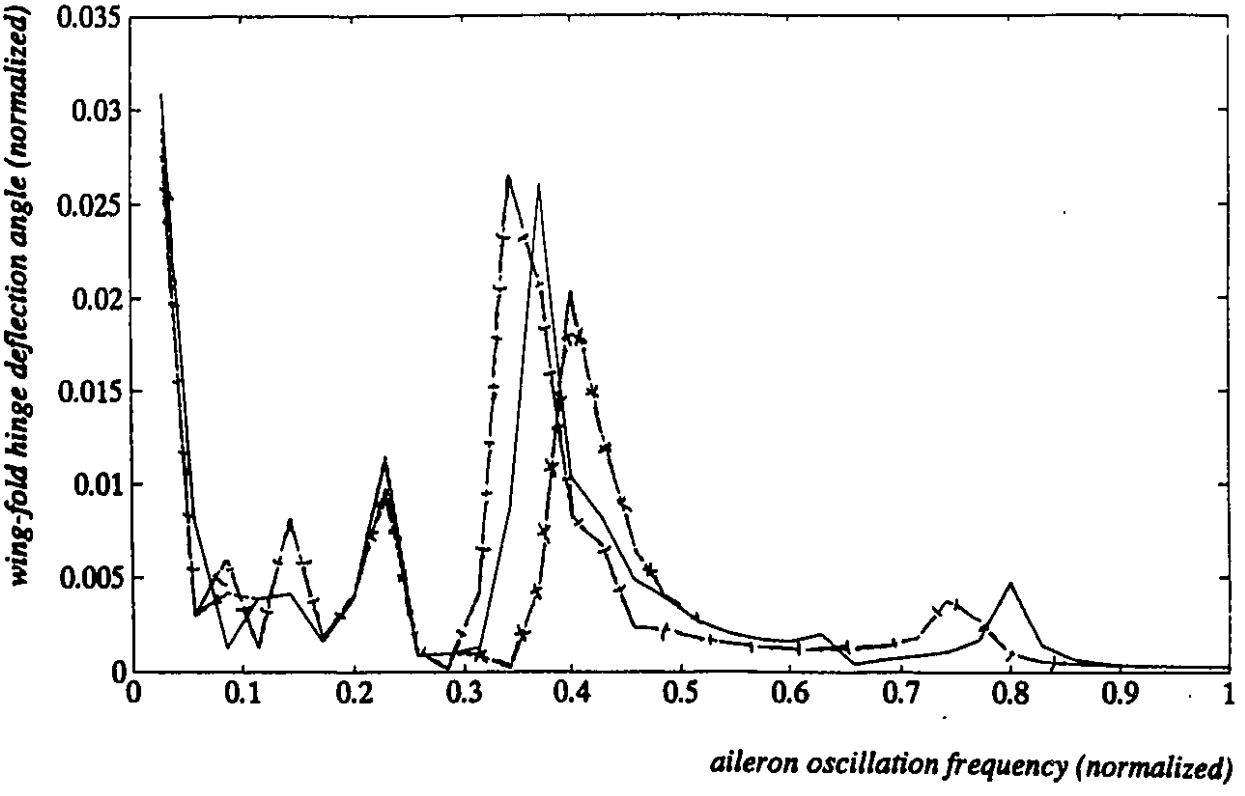

Figure 4.9

Hinge rotation amplitude versus aileron oscillation frequency, for 2 degrees aileron oscillation amplitude, 1.43 V, and

———— *: nonlinear hinge*

—X—X— *: linear hinge, stiffness equal to the nominal hinge stiffness*

—I—I— *: linear hinge, stiffness equal to 75% of the nominal hinge stiffness*

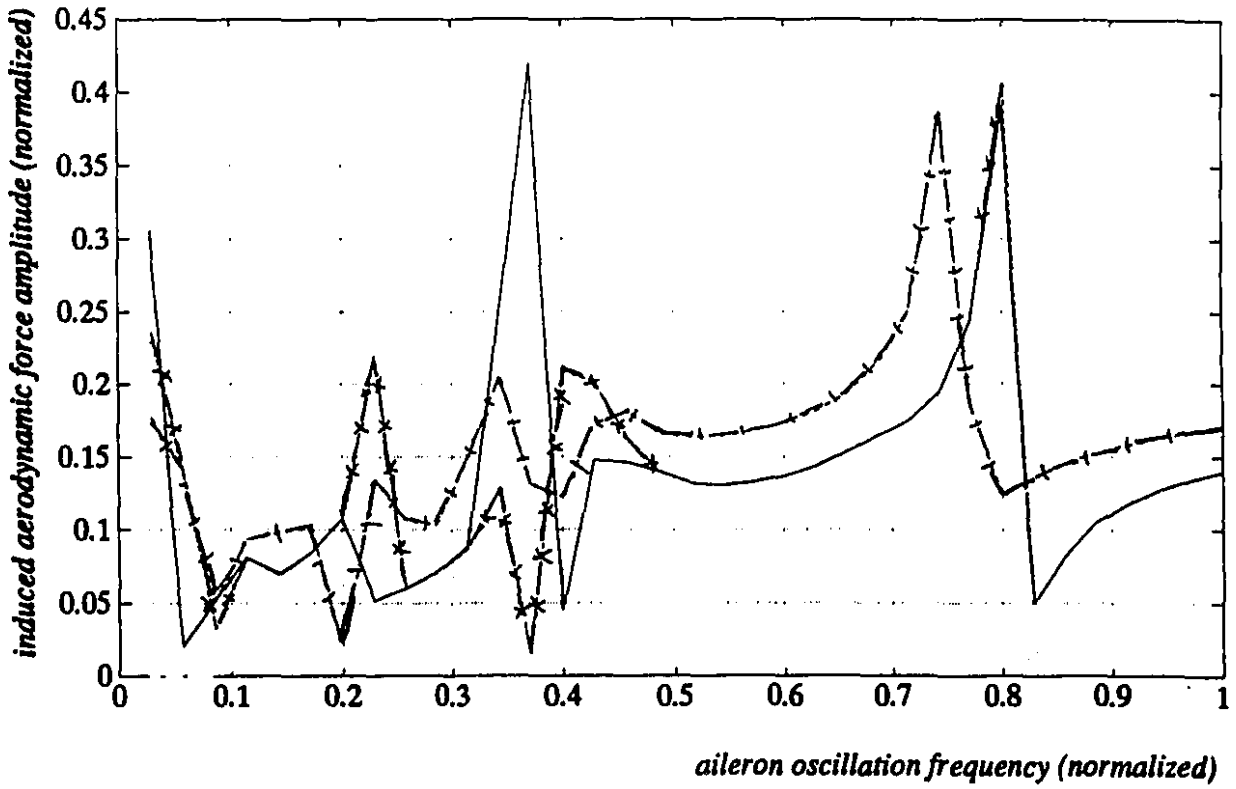

Figure 4.10

Total aerodynamic force versus aileron oscillation frequency, for conditions of Figure 4.9.

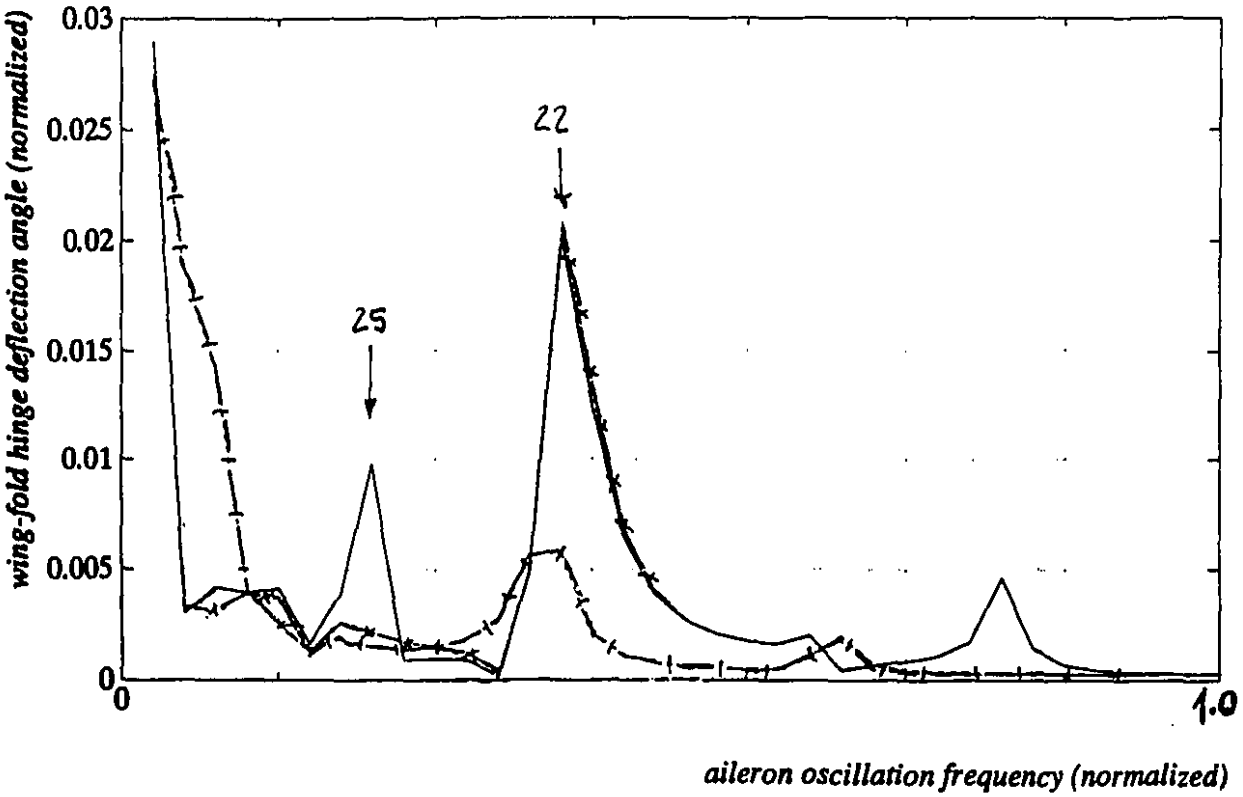

Figure 4.11

Hinge rotation amplitude versus aileron oscillation frequency, for the nonlinear hinge. Calculations are performed progressively taking more modes into account :

——————— *: 25 modes*

—X—X— *: 22 modes*

—|—|— *: 18 modes*

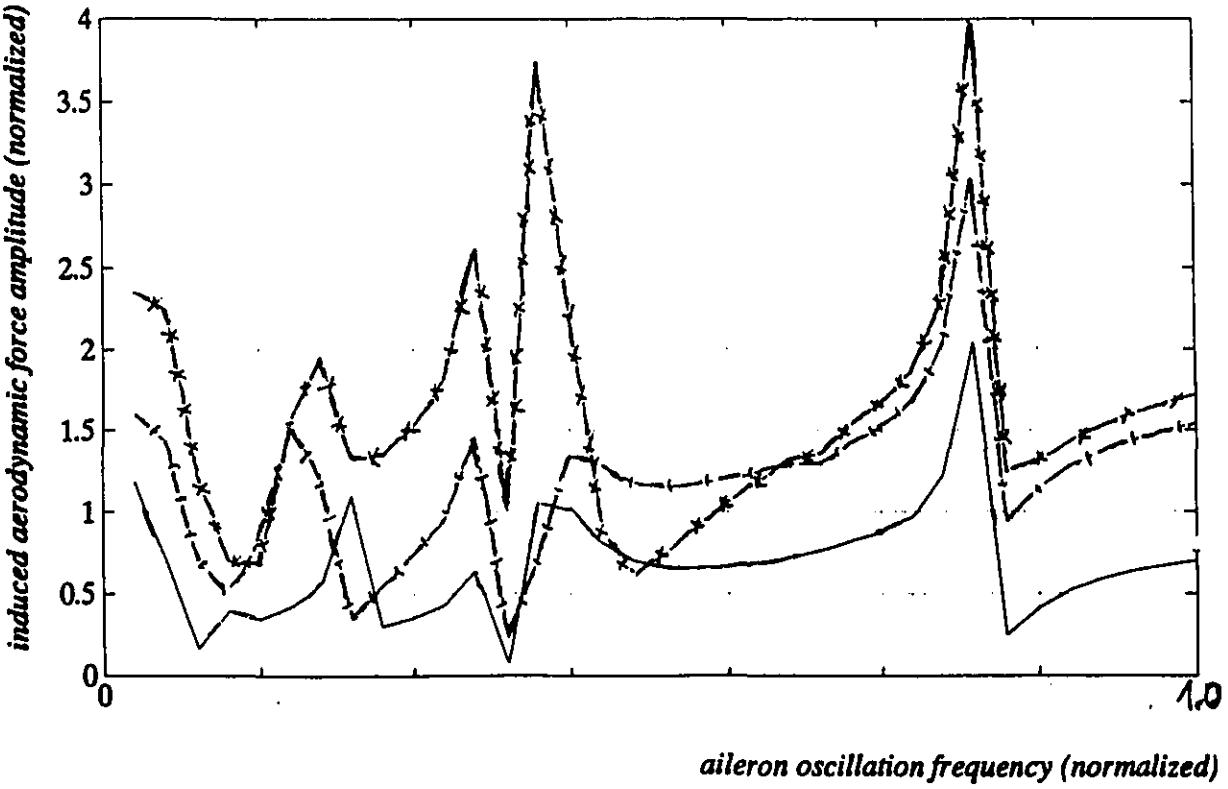

Figure 4.12

Total aerodynamic force versus aileron oscillation frequency, for 18, 22 and 25 modes retained (conditions of Figure 4.11)

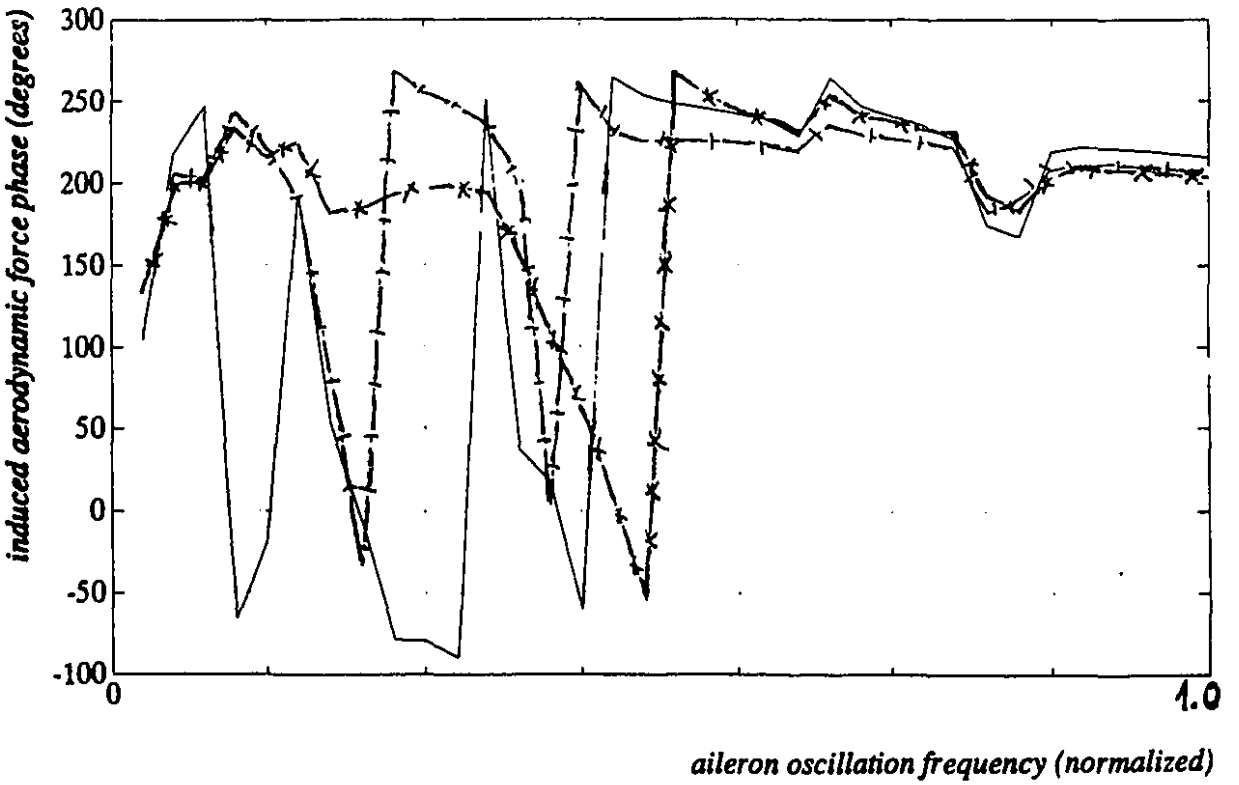

Figure 4.13

Phase lead of aerodynamic force w.r.t. aileron motion, versus aileron oscillation frequency, for 18, 22 and 25 modes retained (conditions of Figure 4.11)

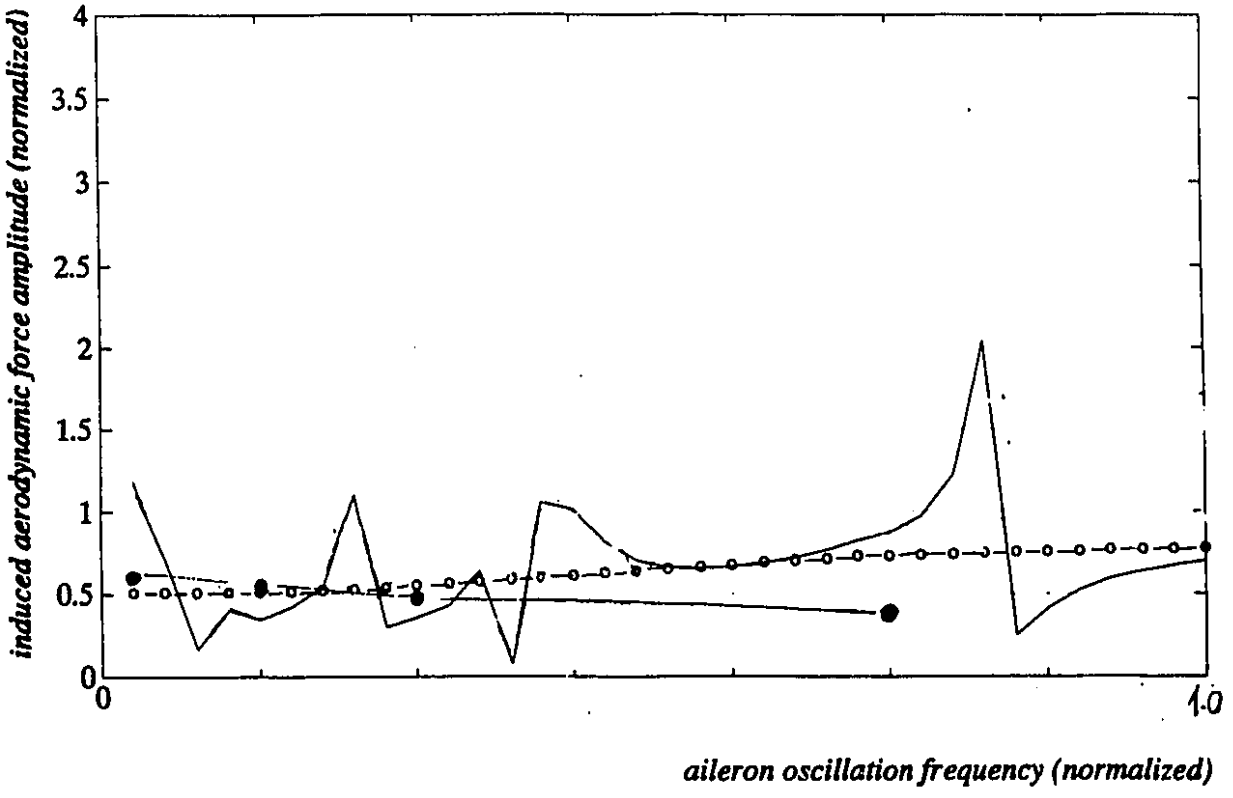

Figure 4.14

Total aerodynamic force versus aileron oscillation frequency, for a flexible and a rigid wing:
——————— : flexible wing (linear wing-fold hinge)
o—o—o— : rigid wing , method 1
●—●—● : rigid wing , method 2

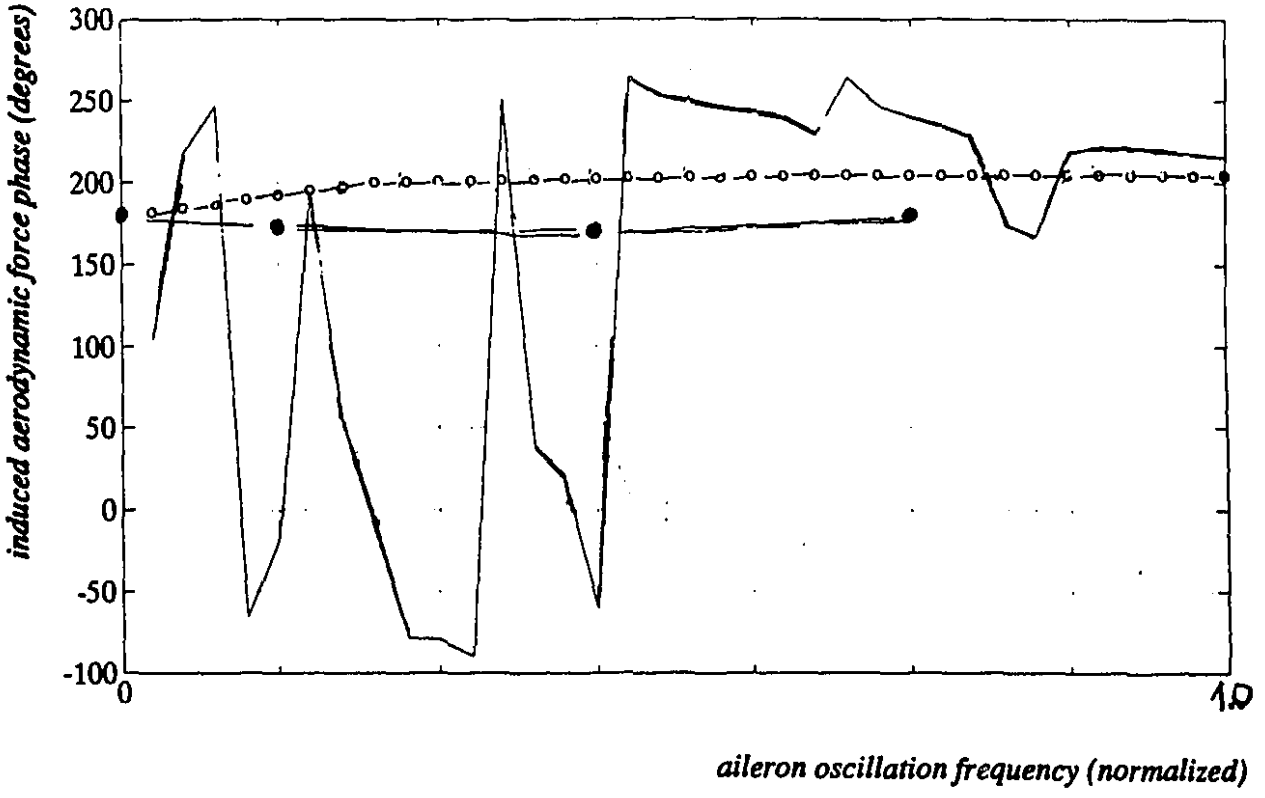

Figure 4.15

Phase lead of the aerodynamic force w.r.t. aileron motion, for conditions of Figure 4.14

Chapter 5

Conclusion

A reasonably complex finite-element model of the wing was used for various analyses. In particular, the effect of the nonlinear wing-fold hinge was taken into account in all analyses.

A limited number of flutter analyses was presented, showing the effect of the wing-fold hinge equivalent stiffness, and compared to more extensive studies on the subject, described in [4].

The main purpose of the thesis was to calculate the response of the wing, with its nonlinear wing-fold hinge, to forced aileron oscillations. The aerodynamic forces induced on the wing due the forced aileron oscillation as well as its own motion were also calculated. The theory needed to perform these calculations was rigourously presented. It extensively relies on transformations between direct equations of motion of the finite-element model of the wing, and the equivalent modal form of the equations. The equations of motion as well as the aerodynamic forces were assumed to be linear. The nonlinear wing-fold hinge was linearized. As the value of the wing-fold hinge equivalent linear stiffness depends on the wing-fold hinge deflection amplitude, the linearization results in a process of iteratively solving sets of linear equations.

An important issue in the solution of the problem is the accuracy of the solution. To limit the cost of the computations, a limited number of modes is considered, rather than retaining all the modes for the calculations. From a theoretical point of view, this is a simplification. It appears that, for flutter analysis, it is justified to assume a very limited number of modes. Chapter 3 showed that modes 4 and 8 were the main fluttering modes. For the problem of forced aileron oscillation however, it was shown that modes beyond the 20-th mode still had considerable and relevant effect on the results.

From the other side, retaining too many modes may adversely affect the accuracy of the solution. Indeed, higher order modes assume complicated mode shapes, and it is reasonable to assume that the accuracy of the induced aerodynamic forces between higher order modes degrades.

In particular, the total aerodynamic force on the wing, due to forced aileron oscillation, was shown to be a value which was very sensitive to the variation of flight parameters, aileron oscillation amplitude and frequency, and the number of modes retained in the equations. This can easily be understood, as the total aerodynamic force is obtained as a sum forces at each of the individual grid points. However, this total aerodynamic force on the wing may not be a very useful variable to calculate. This will depend on the modal identification method used to identify modes from flight tests. It may well be that induced aerodynamic forces at individual grid points (or on regions of the wing) are more relevant values for modal identification, and much less sensitive to parameters of the analysis. The theory presented in the thesis permits to obtain the aerodynamic forces in any of above forms.

Modal identification methods could be studied as an extension to this thesis, and induced aerodynamic forces obtained in accordance with the selected identification method. The graphs obtained in Chapter 4 may also guide the flight tests: choice of an aileron oscillation amplitude, range of frequencies ... Some frequencies show sharp and potentially unreliable peaks, whereas other frequency zones give smoother results. This again

depends on the modal identification method used.

An interesting comparison was made between the results obtained for the flexible wing model, and corresponding results for a wing assumed to be rigid. Considerable differences were shown to occur, very much depending on the wing-fold hinge oscillation frequency.

Linear interpolation was used to interpolate between values of the hard equivalent linear wing-fold hinge stiffnesses, as well as the hard reduced frequencies. I believe that considerable improvement of the results could be obtained by choosing a more refined interpolation method.

Bibliography

[1] E.Albano, W.Rodden: "A Doublet-Lattice Method for Calculating Lift Distributions on Oscillating Surfaces in Subsonic Flows", AIAA Journal, Vol.7 Nr.2, Feb.1969.

[2] H.Katz, F.G.Foppe, D.T.Grossman (McDonnell Aircraft Company): "F-15 Flight Flutter Test Program".

[3] K.Koenig (MBB GmbH, Bremen, Germany): "Problems of System Identification in Flight Vibration Testing".

[4] B.H.K.Lee and A.Tron: "Effects of Structural Nonlinearities on Flutter Characteristics of the CF-18 Aircraft", Aircraft, Vol.26, n8, Aug.1989.

[5] MSC Nastran Theoretical Manual, 1981.